Research Square

Preprints are preliminary reports that have not undergone peer review.
They should not be considered conclusive, used to inform clinical practice,
or referenced by the media as validated information.

The Leisure Economy: The Future of Growth and Population under a Binding Energy Limit

Tobias Bergmann

tobias.bergmann@pik-potsdam.de

Potsdam Institute for Climate Impact Research

Ottmar Edenhofer

Potsdam Institute for Climate Impact Research

Matthias Kalkuhl

Potsdam Institute for Climate Impact Research

Research Article

Keywords: limits to growth, leisure, work time, scarcity rent, Baumol's cost disease, renewable resources, endogenous fertility, population growth

Posted Date: November 4th, 2026

DOI: https://doi.org/10.21203/rs.3.rs-11402514/v1

License: This work is licensed under a Creative Commons Attribution 4.0 International License.
Read Full License

Additional Declarations: No competing interests reported.

The Leisure Economy: The Future of Growth and Population under a Binding Energy Limit*

Tobias Bergmann† Ottmar Edenhofer‡ Matthias Kalkuhl§

October 2026

Abstract

This paper analyzes where productivity gains go when output is bounded but humanity is still innovative. We build a modified Ramsey growth model with endogenous fertility and an endogenous allocation of time between work, leisure and child rearing, in which a renewable resource is essential in production but limited in supply. When the resource constraint binds, the income share of the resource rises and is increasingly captured by a scarcity rent. We denote this pattern as Baumol's Energy Cost Disease. This mechanism decreases the labor share and productivity gains translate into work time reduction and the emergence of a leisure economy. Calibrating our model to the global economy for 1960–2020, we illustrate the quantitative effects for the coming centuries and show that population growth is reduced in anticipation of a resource-constrained economy. The welfare criterion then governs how many people share the bounded output. In two extensions we show that a total utilitarian planner chooses larger populations at lower per-capita consumption, and that the transition mechanisms carry over when endogenizing the research process, provided the energy constraint is reached before ideas run out.

Keywords: limits to growth, leisure, work time, scarcity rent, Baumol's cost disease, renewable resources, endogenous fertility, population growth
JEL codes: E25, J11, J13, J22, O41, O44, Q43

*We would like to thank participants of the Climate Macro Workshop Berlin 2023, the AURÖ Workshop 2024, the SURED 2024, the LAGV 2024, the EAERE 2024 and the VfS Jahrestagung 2024 for helpful comments. We also thank Michael Burda, Simon Dietz, Reyer Gerlagh, Bruno Lanz, Lennart Stern, Michael Sureth, Klaus Prettner and Malin Wiese for valuable feedback and comments.

†Corresponding author. Email: tobias.bergmann@pik-potsdam.de, Potsdam Institute for Climate Impact Research (PIK), P.O. Box 601203, 14412 Potsdam and Technical University Berlin.

‡PIK and Technical University Berlin.

§PIK and University of Potsdam, Faculty of Economic and Social Sciences, Germany.

1 Introduction

What if we live in a zero growth world but humankind is still innovative? Artificial intelligence makes this question less hypothetical than it seems, as it may soon generate new ideas with little human input. Yet output still depends on inputs that ideas cannot multiply. In the weak-links view of Aghion et al. (2017) and Jones (2026), output is then limited by the essential input that cannot be expanded. We study an economy in which this weak link is a renewable resource flow, and ask where productivity gains go when output is bounded.

We follow the intuition of Dasgupta (2021) and model a world in which a renewable resource is essential in production but in limited supply, so that labor productivity gains cannot be turned into proportionately higher production. We embed this resource limit in a Ramsey growth model with endogenous fertility and an endogenous allocation of time between work, leisure and child rearing. Thus, productivity gains can go to three places: higher consumption, more people, or more leisure. Without the limit, work time stays almost constant since income and substitution effects of rising wages largely offset each other in our model. A binding resource limit changes this by constraining ever higher output. Productivity gains then decrease work time, while the welfare criterion decides how many people share the bounded output. Three mechanisms emerge.

First, we find what we call Baumol's Energy Cost Disease. The essential but limited renewable resource (henceforth also just 'energy') in our model is capped in quantity, while productivity in harvesting it continues to grow. Once the limit binds, output grows against a fixed energy flow, so the marginal product of energy and with it its factor share rise. This effect is similar to Baumol's Cost Disease (Baumol, 1967; Baumol & Bowen, 1966; Baumol & De Ferranti, 2012). In Baumol's setting, the share of the stagnant sector grows because its relative price rises, and labor flows into that sector. In our model the same pattern arises from scarcity rather than stagnation, but labor leaves the energy sector as well. We show that for a growing effective workforce the scarcity rent takes over the total factor income of the economy in the long run. This value increase is the textbook definition of a scarcity rent, which in principle can be taxed efficiently without any distortions, as it is the case for land rents (Tideman, 1982). Once the limit binds, redistribution might become less costly if this scarcity rent can be taxed efficiently.

Second, we see the emergence of a leisure economy. As a growing share of income

goes to the scarce resource rather than to labor, the labor share and with it work time fall. The freed time goes to leisure rather than to child rearing, since each additional person must share the fixed resource. The idea of turning productivity gains into work-time reduction goes at least back to Keynes (1930), who speculated about a 15-hour work week within a hundred years. Since we did not see this, Spencer (2023) concludes that Keynes underestimated consumerism and the satisfaction of wants rather than needs. Our model offers a complementary reading. As long as output can grow, productivity gains go to consumption. Once output is bounded, they go to leisure.

Third, resource constraints also influence the population dynamics of the economy. Anticipating that output will eventually be bounded by the renewable resource, the social planner reduces fertility already before the limit becomes binding. Additional population growth would lower consumption per capita once production is constrained, which reduces the value of having additional children. The welfare criterion decides how many people share the bounded output. An average utilitarian planner prefers fewer people with higher consumption per capita. A total utilitarian planner values additional people and accepts lower consumption per person. In the long run, demography also decides whether the limit keeps binding. If population declines faster than energy productivity grows, the limit eventually stops binding.

We calibrate the model to the global economy for 1960–2020 and illustrate the coming centuries. In our baseline, population stays between 9.5 and 11 billion through 2500. The energy limit binds from 2300 onward and by 2500 the scarcity rent already absorbs 18 percent of output. In the long run, population declines slowly, but energy productivity grows faster. The baseline therefore settles in a leisure economy on an empty planet (Jones, 2022a), with a slowly declining population and a permanently binding limit.

We consider two extensions. First, a total utilitarian planner would raise child-rearing time substantially, and population would exceed 200 billion by 2500. Second, we endogenize research, which introduces a second constraint that could end growth. Either ideas run out first, or the energy limit binds first. Whenever the limit binds first, the mechanisms of the baseline carry over. Our baseline can be read as a world in which artificial intelligence generates new ideas without human time input. In such a world, energy and not ideas is the binding constraint. This changes who earns the income of the weak link. In Jones (2026), automation raises the income share of workers who perform the remaining weak links. In our model, the weak link is a natural resource

and its income share accrues as a scarcity rent, which can in theory be taxed without any distortion.

Our model is closest to Jones (2022a), but adds the consumption-leisure trade-off and a renewable resource as an essential and limited input in production. In contrast to most papers in the field (Bretschger, 2020; Gerlagh et al., 2023; Lanz et al., 2017), we study an economy in which the limit actually binds and cannot be circumvented by technological progress, efficiency gains, substitution or structural change. We are, thus, interested in the dynamics of a zero-growth economy regarding factor income, leisure and population. Proponents of degrowth and post-growth frequently call for reductions in work-time (Kallis et al., 2013; Pullinger, 2014) but these are often policy proposals or the call for preference shifts. We argue that work-time reductions naturally evolve once we live in a world with a binding limited essential resource. Lange (2018, p.204) also points out that "in order to achieve zero growth the reduction in average working hours needs to exactly balance out the effect of technological change". Hence, we make the argument the other way around. Living in a renewable resource constrained economy leads to zero-growth, which in turn redirects technological progress into the reduction of working time. Finally, we investigate a *renewable* resource constrained economy. In contrast to the cake eating problem of exhaustible resources (Dasgupta & Heal, 1974; Meadows et al., 1972), renewable resources can guarantee a positive level of consumption in the long run, even though decoupling is not possible. This cannot be overstated since the model economy we envision provides a significant amount of resources enabling humankind to live on a very high material living standard, although aggregate output is constant in the long run. Furthermore, we are not concerned with an open-access renewable resource, for which overuse results in diminishing resources, as in Brander and Taylor (1998). This is a strong assumption since we presume that the renewable resource is managed optimally. In our case, the resource can best be thought of as energy coming from solar panels. Ultimately, when every square meter of the world is covered with the most efficient solar panel, the limit becomes binding.

The rest of the paper is structured as follows. The following section reviews the literature in the field. Section 3 presents the model, while Section 4 derives analytically Baumol's Energy Cost Disease, the leisure economy and the long-run dynamics. Section 5 describes the calibration of the model and Section 6 presents numerical results, including a total utilitarian and endogenous growth extension. Finally, Section 7 concludes.

2 Related Literature

Our paper contributes to three strands of literature: growth models with natural resources, fertility and population economics, and the economics of work-time reductions and leisure. Recent research has increasingly explored the intersection of these fields, particularly the interplay between resource scarcity, climate change, and demographic dynamics.

Within the literature on growth and natural resources, Lanz et al. (2017) introduce a land-constrained growth model to examine the relationship between population growth, land demand, and technological progress. Their framework incorporates a potential Malthusian constraint, although it remains non-binding in their analysis. Our study extends this perspective by explicitly considering scenarios in which such constraints become binding and exploring their economic implications. Burda and Zessner-Spitzenberg (2024) extend the Solow–Swan framework by introducing an environmental constraint on greenhouse gas accumulation and show that, once this limit binds, economic growth requires a permanently expanding mitigation sector. In their model, differences in technological progress across sectors generate a Baumol-type effect, with rising relative prices and reallocation of resources toward abatement activities. Wang et al. (2025) develop a two-sector integrated assessment model with sector-specific climate damages and imperfect substitutability between goods. Asymmetric damages reduce productivity growth in climate-sensitive sectors, raising their relative prices and inducing a climate Baumol disease that slows aggregate output growth. Gerlagh and Van Der Zwaan (2002) provide an early analysis of long-term substitutability between environmental and man-made goods. They show that if these inputs are poor substitutes, long-run growth eventually becomes constrained by the limited availability of environmental resources, leading to increasing natural resource rents — a mechanism they also refer to as a Baumol disease. Our framework complements this insight by showing that, when resource limits constrain further substitution, the adjustment margin shifts from production to leisure, yielding a transition toward a leisure economy rather than continued material expansion.

Further connecting population dynamics with environmental concerns, Gerlagh (2023) develops an endogenous growth model to assess the dual role of population growth in climate change. On the one hand, a larger population exacerbates emissions and climate damages (the congestion view). On the other hand, it accelerates

innovation and the discovery of climate solutions (the innovation view). Their findings underscore the importance of balancing these opposing forces when evaluating the impact of demographic trends on aggregate welfare. Bretschger (2020) incorporates endogenous fertility into a multi-sector growth model with exhaustible resources, physical and knowledge capital, and climate change. His results indicate that, in steady state, climate change remains independent of population growth, as the innovation channel—driven by labor in the research sector dominates resource depletion effects. Investigating endogenous population, Córdoba and Liu (2022) study growth in the presence of a fixed production factor, land. They establish that optimal steady-state population is proportional to both fixed resources and technological progress, while per capita consumption remains independent of these factors. Thus, in their model stagnation in per-capita consumption arises as a socially optimal trade-off between life quality and population size when natural resources are limited. Similarly, Peretto and Valente (2015) investigate the interplay between resource prices and fertility in a Schumpeterian growth model with endogenous fertility. Their results indicate that the response of fertility to resource scarcity depends on the relative increase in resource prices compared to wages and the degree of substitutability between labor and natural resources in intermediate goods production.

Departing from this strand, we argue that the innovation channel is ultimately bounded by natural limits. Thus, we think of an economy in which production relies on an essential and renewable yet finite input, which cannot be improved endlessly. This idea is similar to the model lined out in Bergmann and Kalkuhl (2025, Section 4.2.3).

Jones (2022a) examines the implications of negative population growth for economic performance. He argues that declining fertility and shrinking populations can lead to falling living standards, culminating in what he terms the "empty planet" scenario. Extending this debate, Strulik (2024) argues that even with sub-replacement fertility, sustained growth is feasible as long as human capital continues to accumulate. Strulik and Weisdorf (2008) show that structural change from agriculture to industry can endogenously trigger the demographic transition, while Strulik et al. (2013) demonstrate that, once innovation becomes human-capital-driven, technological progress decouples from population growth.

In the broader field of fertility and population economics, Doepke et al. (2022) provide a comprehensive review, identifying key drivers of fertility transitions over

the past century. They highlight two dominant mechanisms: the quantity-quality trade-off and the opportunity cost of mothers' time. However, they argue that in recent decades, particularly in high-income countries, these traditional explanations have weakened, with factors such as family policies, social norms, and labor market flexibility emerging as new determinants of fertility choices.

Building on the welfare implications of population size, Adhami et al. (2023) adopt a total utilitarian approach to assess the consumption-equivalent benefits of larger populations. They find that, when accounting for population size in social welfare calculations, countries like Mexico and South Africa perform better than their per capita consumption statistics suggest, whereas aging societies like Germany and Japan rank lower due to declining population growth highlighting the crucial role of population levels in welfare assessments.

Dietz and Lanz (2025) develop an integrated structural model that links long-run economic growth with climate change adaptation, explicitly incorporating mechanisms such as structural reallocation between agriculture and non-agriculture, directed technical change, and endogenous fertility. Their research focus lies on the role of adaptation to climate change in the long run and shows that while adaptation, primarily via increased agricultural innovation and reallocation of capital and labor into agriculture, has significantly mitigated the direct negative effects of climate change on crop yields, it has concurrently slowed the broader structural shift away from agriculture. The counterfactual simulations reveal that, in the absence of adaptation, climate damages would have been substantially larger in both agriculture and other sectors, although the cost of adaptation remain non-trivial, especially in the non-agricultural economy.

Turning to the literature on work-time reductions and leisure, Bilancini and D'Alessandro (2012) explore the effects of production, consumption, and leisure externalities in an endogenous growth model. Their analysis reveals that a fully informed social planner would prioritize higher leisure and lower consumption to maximize well-being. Similarly, Saint-Paul (2021) examines the potential for long-run satiation in an endogenous growth framework, showing that decentralized economies may converge to either a "Leisure Society" or a "Consumer Society" equilibrium, even though a social planner would never choose long-run satiation. Complementing this, Fagnart et al. (2023) analyze the effect of work-time reductions in a one-sector Ramsey growth model with unemployment and natural capital. They demonstrate that reducing work hours can boost employment when natural capital is sufficiently scarce, offering a potential policy

avenue for mitigating unemployment in resource-constrained economies.

With this paper, we connect all three strands of the literature by integrating the consumption-leisure trade-off into a resource-constrained economy with endogenous population growth.

3 Model

We build on the concept proposed by Dasgupta (2021), which posits that output is ultimately constrained by the biosphere's regenerative capacity. To simplify this idea, we assume the presence of an essential but finite renewable resource. While this approach abstracts from transitional improvements in resource productivity and assumes optimal resource management, it effectively captures the core notion of an upper bound on regeneration. Our framework serves as a simplified representation of his concept but can be extended to incorporate more complex dynamics, such as non-linear renewable resources or environmental sinks. Ultimately, our focus is on understanding the economic dynamics at this natural limit.

3.1 Model Setup

The essential but limited resource can be used at rate $E(t)$ in each period but is ultimately bounded by $\bar{E}$. Thus, it always holds that

$$E(t) \leq \bar{E}. \tag{1}$$

The renewable resource, henceforth energy, is produced using the capital stock in the energy sector, K_E, and labor time, L_E, such that

$$E(t) = \left(A_E(t) L_E(t) P(t)\right)^{\nu} K_E(t)^{1-\nu}, \tag{2}$$

with ν being the labor share in the energy sector, $A_E(t)$ labor-augmenting total factor productivity, and $P(t)$ the population level.

Final output, $Y(t)$, is produced using a nested constant elasticity of substitution production function of the form

$$Y(t) = F(Z(t), E(t)) = \left(aZ(t)^{\sigma} + bE(t)^{\sigma}\right)^{\frac{1}{\sigma}}, \tag{3}$$

with a the share of the labor-capital composite in production, b the share of the renewable resource in production, σ the substitution parameter derived from the elasticity of substitution, $s = \frac{1}{1-\sigma}$, between the labor-capital composite $Z(t)$ and the renewable resource $E(t)$. The labor-capital composite, $Z(t)$, is given by

$$Z(t) = (A_Z(t)L_Z(t)P(t))^{\alpha}K_Z(t)^{1-\alpha}. \tag{4}$$

$L_Z(t)$ and $K_Z(t)$ are the labor input and capital stock in intermediate good production, $A_Z(t)$ labor-augmenting total factor productivity and α is the share of labor in intermediate production.

Since the renewable resource, is an imperfect substitute in production and cannot be replaced, we assume that the elasticity of substitution is less than one ($s < 1$).[1] The capital stocks, $K_i(t)$ with $i \in \{Z, E\}$, evolve according to

$$\dot{K}_i(t) = I_i(t) - \delta K_i(t), \tag{5}$$

with $I_i(t) \geq 0$ denoting investment in sector i, and δ the depreciation rate. Labor productivity in sector i is exogenously growing, also when the limit becomes binding and evolves according to

$$\dot{A}_i(t) = g_{A_i}A_i(t), \tag{6}$$

with g_{A_i} the exogenous growth rate of labor productivity in sector i. We relax this assumption in Section 6.3, where we discuss the case of endogenous growth. However, this formalization of growth can also be thought of as artificial intelligence being able to develop new ideas on its own without any human input (Aghion et al., 2017). Specifically, new ideas do not require human time commitment and the growth process happens truly exogenously.

[1] An elasticity of substitution between energy and non-energy inputs greater than one implies that, in the long run, production could occur without any energy input. This is clearly at odds with thermodynamic laws (Dasgupta & Heal, 1979, p.211). We also exclude the knife-edge case of $s = 1$. Under a continuous probability distribution over substitution elasticities, the probability of it being exactly one is zero. Empirical studies estimating the short to medium run elasticity also find values lower than one (Bayer et al., 2023; Bretschger & Jo, 2024; Fried, 2018; Fried et al., 2022; Hinkelmann, 2024; Van Der Werf, 2008).

The utility function of the representative agent is given by

$$U(c(t), l(t), n(t)) = \frac{(c(t) - \bar{c})^{1-\eta}\ l(t)^{\gamma(1-\eta)}\ n(t)^{\epsilon(1-\eta)}}{1-\eta} + \bar{u}, \tag{7}$$

where $c(t)$ is consumption per person in period t and $\bar{c}$ is the level of subsistence consumption. $l(t)$ is the share of total time endowment spent on leisure and $n(t)$ is the number of children per period per person. The parameters η, γ and ϵ measure intertemporal inequality aversion, the preference for leisure and the preference for children. This specification of the utility function is similar to King-Plosser-Rebelo preferences (King et al., 2002). It implies that income and substitution effects offset such that work and leisure shares are constant along a balanced growth path. We maintain $\eta > 1$ throughout, so utility is defined for $c > \bar{c}$ and marginal utility diverges as consumption approaches subsistence.

Furthermore, we follow Adhami et al. (2023) and introduce the term $\bar{u}$ to match the value of a year of life, measured in dollars, as a ratio to consumption per person. We do this to ensure that the social planner values population in the social welfare function even if utility expresses a negative sign. The calculation of $\bar{u}$ is described in Section C.1.

Time is normalized to one and divided between working in the intermediate or energy sector, care time for rearing children, and leisure time so that

$$1 = L_Z(t) + L_E(t) + L_n(t) + l(t). \tag{8}$$

Having kids is costly. The household has to invest time, $L_n(t)$, for rearing children. The number of births per person and period t, $n(t)$, is endogenously determined by the amount of time spent rearing children, $L_n(t)$, and given by

$$n(t) = \kappa(t) L_n(t)^{\psi}, \tag{9}$$

with $\kappa(t)$ being a time dependent but exogenous cost parameter and $\psi \in (0, 1]$ capturing diminishing returns in child production.

Population, $P(t)$, evolves endogenously according to

$$\dot{P}(t) = (n(t) - d(t))P(t), \tag{10}$$

where $n(t)$ is given by eq. (9) and $d(t)$ is the time dependent but exogenous mortality rate indicating how many people die each period.

All goods either have to be consumed or invested so it holds that

$$Y(t) = P(t)c(t) + I_Z(t) + I_E(t). \tag{11}$$

The social planner is either total or average utilitarian. This is captured by the parameter $\theta \in [0, 1]$, with $\theta = 0$ indicating average utilitarianism and $\theta = 1$ total utilitarianism. Thus, social welfare is given by

$$W = \int_0^\infty P(t)^\theta \cdot U(c(t), l(t), n(t)) \cdot e^{-\rho t} dt, \tag{12}$$

where ρ is the pure rate of time preference of the social planner. This specification allows us to analyze different normative assumptions on population ethics. The case of $\theta = 0$ also mimics a decentralized economy in which households enjoy their children via $n(t)$ in the utility function but not the size of their dynasty. We focus in the main analysis on the average utilitarian case (Section 6.1), but discuss, as a thought experiment, how the optimal path changes if the planner adopts total utilitarianism from today onward (Section 6.2). The model environment is summarized in Table 2.

3.2 Social Planner Solution

The social planner maximizes social welfare by choosing consumption, capital, population and the amount of work and care time

$$\max_{\{c(t), K_Z(t), K_E(t), I_Z(t), I_E(t), P(t), L_Z(t), L_E(t), L_n(t)\}} \int_0^\infty P(t)^\theta U(c(t), l(t), n(t)) e^{-\rho t} dt. \tag{13}$$
$$\text{s.t.} \quad (1) - (11)$$

Table 1: Economic Environment

Final output	$Y = (aZ^{\sigma} + bE^{\sigma})^{\frac{1}{\sigma}}$
Intermediate goods	$Z = (A_Z P L_Z)^{\alpha} K_Z^{1-\alpha}, \quad E = (A_E P L_E)^{\nu} K_E^{1-\nu}$
Population	$\dot{P} = (n-d)P$
Fertility	$n = \kappa L_n^{\psi}$
Utility	$U(c,l,n) = \frac{(c-\bar{c})^{1-\eta} l^{\gamma(1-\eta)} n^{\epsilon(1-\eta)}}{1-\eta} + \bar{u}$
Time constraint	$1 = L_Z + L_E + L_n + l$
Consumption	$cP = Y - I_Z - I_E$
Welfare	$W = \int_0^{\infty} P^{\theta} \cdot U(c,l,n) \cdot e^{-\rho t} dt$

From this we can set-up the current value Hamiltonian

$$\begin{aligned}
\mathcal{H} &= P(t)^{\theta} U(c(t), 1 - L_Z(t) - L_E(t) - L_n(t), n(t)) \qquad (14)\\
\text{Resource:} \quad &- \lambda(t)\Big(E(t) - \bar{E}\Big)\\
\text{Output:} \quad &+ \mu_Y(t)\Big(Y(t) - c(t)P(t) - I_Z(t) - I_E(t)\Big)\\
\text{Intermediate Capital:} \quad &+ \mu_Z(t)\Big(I_Z(t) - \delta K_Z(t)\Big)\\
\text{Energy Capital:} \quad &+ \mu_E(t)\Big(I_E(t) - \delta K_E(t)\Big)\\
\text{Population:} \quad &+ \mu_P(t)\Big((n(t) - d)P(t)\Big),
\end{aligned}$$

where $\lambda(t)$ denotes the shadow price of relaxing the upper bound on energy use, $\mu_Y(t)$ is the multiplier on the aggregate resource constraint, and $\mu_Z(t)$, $\mu_E(t)$, and $\mu_P(t)$ represent the current-value shadow prices of capital in the intermediate sector, capital in the energy sector and population, respectively. In the optimum the three goods multipliers coincide, $\mu_Y = \mu_Z = \mu_E$, since investment can be reallocated freely. The detailed derivations can be found in Section A.

Optimization results in five optimality conditions. The optimality conditions for the

intermediate goods sector are well-known results of a simple Ramsey model. Namely the Euler-equation and the consumption-leisure trade off given by

$$F_{K_Z} - \delta - \rho = (1-\theta)\frac{\dot{P}}{P} - \frac{\dot{U}_c}{U_c}, \tag{15}$$

$$F_{L_Z} = -\frac{U_{L_Z}}{U_c}P = \frac{U_l}{U_c}P. \tag{16}$$

The optimality conditions in the energy sector have the same structure but have an additional term capturing the evolution of the scarcity rent once the limit becomes binding

$$F_{K_E} - \delta - \rho = (1-\theta)\frac{\dot{P}}{P} - \frac{\dot{U}_c}{U_c} + \lambda\frac{E_{K_E}}{P^{\theta-1}U_c}, \tag{17}$$

$$F_{L_E} = \frac{U_l}{U_c}P + \lambda\frac{E_{L_E}}{P^{\theta-1}U_c}, \tag{18}$$

with $\lambda(t)(E(t) - \bar{E}) = 0$ and $\lambda(t) \geq 0$. The two conditions preserve the standard structure of optimal input allocation but include an additional term that captures the scarcity rent once the energy constraint becomes binding. In the absence of the cap ($\lambda = 0$), capital and labor in the energy sector are chosen such that their marginal products equal the relevant marginal rates of substitution. When the limit binds ($\lambda > 0$), however, energy is fixed in quantity but not freely available: it must be captured using capital and labor inputs. Productivity gains via increasing A_Z and A_E cannot raise total energy supply beyond $\bar{E}$, but now reduce the amount of inputs required to harvest the fixed resource stock. The additional terms $\lambda\frac{E_{K_E}}{P^{\theta-1}U_c}$ and $\lambda\frac{E_{L_E}}{P^{\theta-1}U_c}$ raise the marginal product that inputs in the energy sector must earn. With diminishing returns, the inputs used for providing the fixed energy endowment are decreased.

The last optimality condition describes the path for optimal population growth given by

$$\theta\frac{\dot{P}}{P} + \frac{\dot{U}_{L_n}}{U_{L_n}} + (1-\psi)\frac{\dot{L}_n}{L_n} - \frac{\dot{\kappa}}{\kappa} = \rho + \kappa\psi L_n^{\psi-1}\frac{U_c}{U_{L_n}}\left(\theta\frac{U}{U_c} + F_P - c - \lambda\frac{E_P}{P^{\theta-1}U_c}\right). \tag{19}$$

The left-hand side of Equation (19) determines the dynamic evolution of the shadow value of child-rearing. It combines four elements: (i) the effect of population growth on welfare weights, governed by θ; (ii) changes in the marginal utility cost of rearing children; (iii) the adjustment term $(1-\psi)\dot{L}_n/L_n$, which captures diminishing returns

in fertility production; and (iv) the term $-\dot{\kappa}/\kappa$, which arises because the fertility technology $\kappa(t)$ is itself changing. While the time cost of children is still rising ($\dot{\kappa} < 0$), postponed fertility increases the cost of children, which adds to the return required from fertility today. When $\psi < 1$, additional time devoted to children reduces the marginal productivity of further child-rearing, thereby affecting the dynamic trade-off.

The right-hand side represents the required return to fertility. Analogous to the Euler equation this return equals the pure rate of time preference, ρ, plus four components that are normalized into utility terms via $\kappa\psi L_n^{\psi-1}\frac{U_c}{U_{L_n}}$.

1. $\theta\frac{U(\cdot)}{U_c}$: Value of statistical life year.
2. F_P: Marginal product of one additional member of society.
3. c: The consumption an additional member of society absorbs.
4. $\frac{\lambda E_P}{P^{\theta-1}U_c}$: Term capturing the scarcity rent.

First, for $\theta > 0$ the value of a statistical life year raises the shadow value of an additional person: a total utilitarian planner counts every new member of society. For $\theta = 0$ the criterion does not count added lives and the term drops out.

Second, the marginal product of one additional member of society raises the shadow value as well, since more people produce more goods and services.

Third, per-capita consumption lowers the shadow value, since an additional person absorbs resources that others could have consumed. This effect is also described in Lanz et al. (2017, p.979).

Lastly, the scarcity rent term lowers the shadow value: the constrained resource has to be shared among more people. Resource constraints therefore influence population dynamics negatively. Since eq. (19) is dynamic, resource constraints already influence the fertility decision today even though the binding date is still far in the future. We illustrate this effect in the numerical simulation in Section 6.1.

3.3 Characterization of the Optimum

The optimal allocation is described by the aforementioned optimality conditions Equations (15) to (19) together with the three differential equations for population and

capital

$$\dot{P}(t) = \big(n(t) - d(t)\big)P(t), \tag{20}$$

$$\dot{K}_Z(t) = I_Z(t) - \delta K_Z(t), \tag{21}$$

$$\dot{K}_E(t) = I_E(t) - \delta K_E(t), \tag{22}$$

the aggregate resource constraint

$$Y(t) = c(t)P(t) + I_Z(t) + I_E(t), \tag{23}$$

the scarcity constraint, and the equations for exogenous technological progress

$$\lambda(t)\big(E(t) - \bar{E}\big) = 0, \qquad \lambda(t) \geq 0, \qquad E(t) \leq \bar{E}, \tag{24}$$

$$A_Z(t) = A_{Z,0} \cdot e^{g_{A_Z} t}, \tag{25}$$

$$A_E(t) = A_{E,0} \cdot e^{g_{A_E} t}. \tag{26}$$

Thus, the optimum is given by a combination of the twelve variables $c(t)$, $K_Z(t)$, $K_E(t)$, $I_Z(t)$, $I_E(t)$ $P(t)$, $L_Z(t)$, $L_E(t)$, $L_n(t)$, $\lambda(t)$, $A_Z(t)$ and $A_E(t)$ solving the twelve Equations (15) to (26), together with the initial conditions $K_Z(0)$, $K_E(0)$, $P(0)$ and the transversality conditions in Section A.

4 Analytical Results

We now characterize the main mechanism of the economy under a binding energy constraint. Two results follow. First, the economy develops Baumol's Energy Cost Disease: the share of income paid to energy rises, and within this share an ever larger part accrues as a pure scarcity rent rather than as wages or capital income. Second, the scarcity rent rises at the expense of factor income. Thus, a smaller share of output is paid for work, and the ratio of work to leisure falls: this is the emergence of the leisure economy. The driving force behind both results is that a binding cap does not stop technological progress: the energy flow is fixed, but productivity keeps growing in both sectors. As long as productivity in the intermediate sector grows faster than the population shrinks, output keeps growing against the fixed flow and the below-unity substitution elasticity of energy makes its share of income rise. If productivity in the energy sector also outruns population decline, ever less capital and labor are

needed to provide the fixed energy flow. Since population is determined endogenously, both conditions depend on the planner's fertility choice. Finally, we characterize the population dynamics in the long run.

4.1 Baumol's Energy Cost Disease

The factor income shares of the intermediate good and energy are given by

$$s_Z(t) = \frac{F_Z(t)Z(t)}{Y(t)} = a\Big(\frac{Z(t)}{Y(t)}\Big)^{\sigma}, \tag{27}$$

$$s_E(t) = \frac{F_E(t)E(t)}{Y(t)} = b\Big(\frac{E(t)}{Y(t)}\Big)^{\sigma}, \tag{28}$$

which sum to one by constant returns. At the cap, $E(t) = \bar{E}$ is fixed, so the energy share $s_E = b(\bar{E}/Y)^{\sigma}$ rises whenever output grows, and the intermediate share falls one for one. As Z accumulates against the fixed flow, each additional unit of the intermediate is worth less at the margin, while each unit of energy is worth more. The share of income paid to the factor that cannot expand rises with output. This is Baumol's Energy Cost Disease.

To see who is paid this rising share, we define the wage, the rental rate of capital and the scarcity rent as shadow prices of the planner's problem:

$$w(t) \equiv F_{L_Z}(t) = \frac{U_l(t)}{U_c(t)}P(t), \tag{29}$$

$$r(t) \equiv F_{K_Z}(t) = \rho + \delta + (1-\theta)\frac{\dot{P}(t)}{P(t)} - \frac{\dot{U}_c(t)}{U_c(t)}, \tag{30}$$

$$q(t) \equiv \frac{\lambda(t)}{P(t)^{\theta-1}U_c(t)}. \tag{31}$$

Comparing eqs. (16) and (18) and eqs. (15) and (17), labor and capital have the same opportunity cost in both sectors. Without the cap ($\lambda = 0$), their marginal products are therefore equal. With the cap, inputs in the energy sector must also cover the scarcity term. The rent q is the multiplier on the energy constraint expressed in units of output, and it is positive only when the cap binds. The marginal products of labor

and capital in the energy sector can then be rewritten as

$$F_{L_E}(t) = w(t) + q(t)E_{L_E}(t), \tag{32}$$

$$F_{K_E}(t) = r(t) + q(t)E_{K_E}(t). \tag{33}$$

Inserting eqs. (32) and (33) into the energy share identity $s_E = F_{L_E}L_E/Y + F_{K_E}K_E/Y$ yields

$$s_E(t) = \underbrace{\frac{w(t)L_E(t)}{Y(t)}}_{\text{labor: } s_{L_E}} + \underbrace{\frac{r(t)K_E(t)}{Y(t)}}_{\text{capital: } s_{K_E}} + \underbrace{\frac{q(t)E(t)}{Y(t)}}_{\text{scarcity rent: } s_R}. \tag{34}$$

The energy share splits into factor shares for labor, capital and the scarcity rent. We now show when the scarcity rent share rises at the expense of factor income. By log-differentiating the energy technology $\bar{E} = (A_E L_E P)^{\nu} K_E^{1-\nu}$ we obtain a restriction on the growth rates of the two inputs

$$\nu\, g_{L_E} + (1-\nu)\, g_{K_E} = -\nu\, G, \qquad G \equiv g_{A_E} + g_P, \tag{35}$$

where g_x denotes the growth rate of a variable x throughout. The term G is the growth rate of the effective energy workforce $A_E P$. Whenever $G > 0$, a weighted average of the two input growth rates is negative, so at least one input must decline. Ever less of the effective input bundle is needed to provide the fixed energy flow. Which input declines depends on the factor prices. We can rearrange the optimality conditions in the energy sector (32) and (33) to obtain

$$wL_E = \nu\bar{E}(F_E - q), \tag{36}$$

$$rK_E = (1-\nu)\bar{E}(F_E - q). \tag{37}$$

Taking growth rates of the ratio shows that the two payments grow at the same rate, so the input growth rates differ only through factor prices

$$g_{K_E} - g_{L_E} = g_w - g_r \equiv D. \tag{38}$$

Using this in Equation (35) gives us two equations showing how labor and capital in

the energy sector evolve

$$g_{L_E} = -\nu G - (1-\nu)D, \tag{39}$$

$$g_{K_E} = -\nu(G - D). \tag{40}$$

When wages grow faster than capital costs, $D > 0$, the planner substitutes toward capital. Thus, for $G > 0$, energy labor falls while energy capital can still grow if $D > G$. However, if the growth of the effective energy workforce exceeds the price differential, $G > D$, energy capital shrinks; for $-\frac{\nu}{1-\nu}G < D < G$, capital and labor shrink together.

The scarcity rent share within the energy share increases when the energy share grows faster than the combined labor and capital shares

$$g_{(s_{L_E}+s_{K_E})} < g_{s_E}. \tag{41}$$

The growth rate of the energy share is obtained by log-differentiating $s_E = \frac{F_E \bar{E}}{Y}$ and using that the marginal product of energy is given by $F_E = b\bar{E}^{\sigma-1}Y^{1-\sigma}$ so that

$$g_{s_E} = g_{F_E} - g_Y = -\sigma g_Y. \tag{42}$$

The growth rate of the capital and labor share in the energy sector is obtained by log-differentiation of $s_{L_E} + s_{K_E} = \frac{wL_E + rK_E}{Y}$ and using eqs. (36) and (37) to obtain

$$g_{(s_{L_E}+s_{K_E})} = g_w + g_{L_E} - g_Y. \tag{43}$$

Inserting (42) and (43) in (41) gives

$$g_{L_E} + g_w < (1-\sigma)\, g_Y. \tag{44}$$

By imposing an equal labor share in the energy and intermediate goods production, $\alpha = \nu$, and using (38) and (39), together with $g_w = g_{s_Z} + g_Y - g_{L_Z}$, $g_r = g_{s_Z} + g_Y - g_{K_Z}$, $g_{s_Z} = \sigma(g_Z - g_Y)$, $g_Z = \nu(g_{A_Z} + g_{L_Z} + g_P) + (1-\nu)g_{K_Z}$, and $1 - \sigma = 1/s$, we can rearrange this expression to obtain

$$g_Z \;>\; s\nu\,(g_{A_Z} - g_{A_E})\,. \tag{45}$$

The scarcity rent share within the energy share increases exactly when the growth of the intermediate good is greater than the productivity growth differential between the sectors times the elasticity of substitution, s, and the labor share, ν. Since $s\nu < 1$, the scarcity rent share grows whenever the intermediate good grows at least as fast as intermediate productivity A_Z alone. If energy productivity keeps pace with intermediate productivity, $g_{A_E} \geq g_{A_Z}$, the scarcity rent share increases whenever the intermediate good grows at all.

4.2 The Emergence of the Leisure Economy

The allocation of time is governed by the ratio of work to leisure,

$$k \equiv \frac{L_Z + L_E}{l}. \tag{46}$$

We show that this ratio is decreasing in the scarcity rent share. Work time can be rewritten by using the factor-payment identities[2]

$$\frac{wL_Z}{Y} = \alpha s_Z, \quad \frac{wL_E}{Y} = \nu(s_E - s_R), \tag{47}$$

where $s_R \equiv q\bar{E}/Y$ is the scarcity rent share from Equation (34). With $\alpha = \nu$, and using $s_Z + s_E = 1$, summing the two labor incomes gives

$$L_Z + L_E = \frac{\nu\,(1 - s_R)}{w}\,Y. \tag{48}$$

The rent reduces the labor income share, and with it work time. Using the derivatives of the utility function in the wage definition (29) gives $w = \gamma P(c - \bar{c})/l$. This term is strictly positive because marginal utility diverges at subsistence and at zero leisure, so the planner keeps $c > \bar{c}$ and $l > 0$ at every date. Using this and (48) in (46) we obtain the work-leisure ratio

$$k = \frac{\nu\,(1 - s_R)}{\gamma\, s_C}, \qquad s_C \equiv \frac{(c - \bar{c})P}{Y}, \tag{49}$$

[2]From the Cobb-Douglas composite, $w \equiv F_{L_Z} = F_Z\,\alpha Z/L_Z$, so $wL_Z = \alpha F_Z Z = \alpha s_Z Y$; the energy-sector identity follows from (36) with the definitions of s_E and s_R.

with s_C the share of output consumed above subsistence. Together with the time constraint (8), k pins down leisure and total work time, given child-rearing time:

$$l = \frac{1 - L_n}{1 + k}, \qquad L_Z + L_E = \frac{k\,(1 - L_n)}{1 + k}. \tag{50}$$

The higher the scarcity rent share, the lower the work-leisure ratio, k. Work and leisure both scale with $1 - L_n$, so for a given child-rearing time every hour cut from work becomes an hour of leisure. This is the emergence of the leisure economy. This conclusion, however, requires consumption above subsistence. If $(c - \bar{c})P$ falls toward zero, the wage collapses together with the consumption share, and work time need not decline.

4.3 Population Dynamics in the Long Run

We have seen that Baumol's Energy Cost Disease and the leisure economy are driven by growth. Specifically, growth in the effective workforce, consisting of population and technological progress, increases the rent share and reduces work time. Historically, population levels have been rising, which would have strengthened the described effects. Population growth rates, however, are shrinking, and population is projected to decrease in the future. A smaller population takes pressure off the binding cap, and if population declines faster than technological progress advances, the effects driving Baumol's Energy Cost Disease and the leisure economy might reverse. We therefore now look at the long-run population dynamics and test what condition must be met so that a stationary population is consistent with the planner's optimality conditions.

Three settled futures are possible: (i) a leisure economy with a stationary population, in which the welfare criterion decides how many people share the bounded output; (ii) a leisure economy with an ever-declining population, in which consumption per capita increases with the rate of population decline, the empty planet result of Jones (2022a); (iii) an even stronger population decline, outrunning productivity increases in the energy sector, such that energy inputs must increase again to provide the fixed flow and the cap eventually stops binding.[3]

To make statements about the long run, we define a *capped balanced growth path* (capped BGP): a path on which the cap binds from some date onward and every growth

[3] A permanently growing population is not feasible once the cap binds. Bounded output $\bar{Y}$ and the subsistence level $\bar{c}$ limit population to $\bar{Y}/\bar{c}$. Population can grow during the transition, but it can at most converge to a stationary level in the long run.

rate and factor price converges to a constant as $t \to \infty$, so the path is asymptotically balanced, with strictly positive limits for the wage and the rental rate. We can then establish the following lemma:

Lemma 1. *Consider a capped BGP with $g_{A_Z} \geq g_{A_E}$, and let $G = g_{A_E} + g_P$ from (35) denote the growth rate of the effective energy workforce.*

(i) If $\lim_{t\to\infty} G > 0$, the full leisure economy emerges: $s_Z \to 0$ and $Y \to \bar{Y} = b^{1/\sigma}\bar{E}$, all four inputs and work time vanish with $l \to 1 - \lim_{t\to\infty} L_n$, the rent absorbs the energy share with $s_R \to 1$ and $q \to b^{1/\sigma}$, and $C \to \bar{Y}$.

(ii) If $\lim_{t\to\infty} G < 0$, no capped BGP exists: the effective energy workforce falls below the floor required to provide the fixed flow, and the cap ceases to bind in finite time.

Proof. See Section B. □

If the effective energy workforce, consisting of technological progress and population, grows forever, the full leisure economy emerges: output converges to its bound $\bar{Y}$, the scarcity rent captures the entire income, work time has vanished, and the remaining time is split between leisure and child rearing. If instead population declines faster than energy productivity advances, the cap eventually stops binding, future (iii) of the list above. Thus, the long run depends on the endogenous rate of population growth.

Population dynamics are determined by the optimality condition for population stated in (19). We now evaluate this equation on a capped BGP. Two demographic limits complete the setting. Mortality cannot fall forever, and since the time a child requires is bounded, the fertility cost cannot rise forever. We therefore assume that both approach constants eventually,

$$\lim_{t\to\infty} d(t) = \bar{d} > 0, \qquad \lim_{t\to\infty} \kappa(t) = \bar{\kappa} > 0. \tag{51}$$

We now test stationary population: suppose the planner holds population stationary from some date onward. Replacement then requires $n = \bar{d}$, and two long-run values follow,

$$L_n^* = \left(\frac{\bar{d}}{\bar{\kappa}}\right)^{1/\psi}, \qquad l^* = 1 - L_n^*. \tag{52}$$

To achieve a stationary population in the long run the social planner has to set child-rearing time according to (52). On a capped BGP this then also results in leisure absorbing the remainder of the time endowment, since work time vanishes by case (i) of Lemma 1. By inserting the marginal utilities and factor payments into (19) and using eqs. (51) and (52) on a capped BGP we can rearrange the optimality condition for population to obtain

$$c - \theta \frac{U}{U_c} = R\,(c - \bar{c}), \qquad R \equiv \frac{\rho}{\psi\,\bar{d}} \left[\epsilon\psi - \gamma \frac{L_n^*}{1 - L_n^*} \right]. \tag{53}$$

The left side of (53) is the net cost of an additional person: the amount of goods and services a person consumes minus the value of the person's existence. The right side is the utility return on child-rearing time that a stationary population requires. The replacement value R measures what the planner is willing to pay for a stationary population. The bracket describes the utility gain from additional children minus the opportunity cost of foregone leisure time. The prefactor $\rho/(\psi\bar{d})$ accounts for how much time it takes to keep one person in the population: when mortality is high, more births are needed, and when ψ is small, extra child rearing time yields few extra births. The discount rate ρ compares the one-time joy of child-rearing in the utility function with the permanent consumption cost of a person. We can now establish the following proposition:

Proposition 1. *Consider a capped BGP with $\eta > 1$, $\bar{u} > 0$, $g_{A_Z} \geq g_{A_E} > 0$, and demographic limits (51) with $\bar{d} < \bar{\kappa}$.*

1. Stationary population. *Every stationary capped BGP is the full leisure economy of Lemma 1 with $P^* = \bar{Y}/c^*$.*

   (a) *For $\theta = 0$: consistent with the optimality conditions if and only if $R > 1$. The long-run consumption level is $c^* = \bar{c}\,R/(R-1)$.*

   (b) *For $\theta > 0$: consistent for every R, at a unique $c^* > \bar{c}$; no capped BGP with declining population exists.*

2. Declining population. *If $\theta = 0$ and $R < 1$, on any capped BGP fertility settles at the unique root $\hat{L}_n < L_n^*$ of*

$$\epsilon\psi - \gamma \frac{L_n}{1 - L_n} = \frac{\psi\,\bar{\kappa}\,L_n^{\psi}}{\rho + (\eta - 1)\big(\bar{d} - \bar{\kappa} L_n^{\psi}\big)} \tag{54}$$

and population declines at $\hat{g}_P = \bar{\kappa}\hat{L}_n^{\psi} - \bar{d} < 0$.

(a) *If* $\lim_{t\to\infty} G = g_{A_E} + \hat{g}_P > 0$*: the full leisure economy emerges and per-capita consumption grows at the rate of population decline* $-\hat{g}_P$.

(b) *If* $\lim_{t\to\infty} G = g_{A_E} + \hat{g}_P < 0$*: case (ii) of Lemma 1: no capped BGP exists, and the cap eventually unbinds.*

Proof. See Section B. □

The average utilitarian social planner sustains a stationary population if R exceeds one: the joy of raising children must cover the goods and services an additional person consumes. If R falls below one, the planner instead prefers slightly fewer people at slightly higher consumption at every date. Fertility settles below replacement, population declines without limit, and consumption per capita grows at the rate of population decline: this is the empty planet result of Jones (2022a). As long as the effective energy workforce keeps growing, the empty planet remains a leisure economy. If population declines faster than energy productivity increases, the cap eventually unbinds and no capped BGP exists.

A total utilitarian social planner never chooses the empty planet scenario. The value of a statistical life year eventually grows faster than the consumption an additional person absorbs. Thus, for any R the total utilitarian social planner holds population stationary. The resulting consumption per capita is above the subsistence level $\bar{c}$, since consumption falling towards subsistence also reduces utility per person: at some point adding another person reduces welfare. However, the higher the existence value $\bar{u}$, the higher the value of an additional person and the larger the stationary population at lower consumption per capita.

5 Calibration

This section presents a calibrated version of the model to illustrate the mechanisms described in the previous section. We distinguish between external calibration, where parameters are fixed based on empirical evidence or literature values, and internal calibration, where parameters are chosen to reproduce key empirical moments of GDP per capita, population, fertility, and energy intensity. Table 3 summarizes our parameter choices.

Table 3: Model Parameters

Description	Symbol	Value	Comment
External Calibration			
Pure rate of time preference	ρ	0.01	Drupp et al. (2018)
Inequality aversion	η	1.35	Drupp et al. (2018)
Utility of existence	$\bar{u}$	12.8	Section C.1
Fertility preference parameter	ϵ	1	Normalization
Subsistence consumption	$\bar{c}$	0.365	One USD per day
Depreciation rate	δ	0.1	Standard macro value
Labor share in intermediate sector	α	0.6	Corresponds to observed labor share
Labor share in energy sector	ν	0.6	Symmetry with intermediate sector
Share of intermediate composite	a	0.9	Implied by energy share
Share of energy in production	b	0.1	Observed energy share
Initial child-rearing cost (1960)	κ_0	0.055	Own calibration, Section C.2
Long-run child-rearing cost	$\bar{\kappa}$	0.015	Own calibration, Section C.2
Growth rate of child-rearing cost	g_κ	0.018	Own calibration, Section C.2
Initial death rate (1960)	d_0	0.016	Own calibration, Section C.2
Decline rate mortality	g_d	0.024	Own calibration, Section C.2
Steepness first mortality transition	m_1	0.04	Own calibration, Section C.2
Midpoint first mortality transition	t_1	79	Own calibration, Section C.2
Death rate at UN projection horizon	d_{UN}	0.0125	Own calibration, Section C.2
Long-run death rate (scenario)	$\bar{d}$	0.008	Scenario value
Steepness second mortality transition	m_2	0.05	Smooth transition, Section C.2
Midpoint second mortality transition	t_2	200	Smooth transition, Section C.2
Initial population (billions)	P_0	3	United Nations (2022)
Energy scaling parameter	ϕ_E	13.4	Matches 1960 energy intensity
Upper bound on energy inflow	$\bar{E}$	10,000	Technical potential (EJ)
Internal Calibration			
Leisure preference parameter	γ	0.818	Calibrated to 2006 US leisure share
Initial Z-capital stock	$K_{Z,0}$	22.5	Matches 1960 output
Initial energy capital stock	$K_{E,0}$	2.5	Matches 1960 output
Initial productivity (intermediate)	$A_{Z,0}$	5	Matches 1960 output
Initial productivity (energy)	$A_{E,0}$	180	Matches 1960 energy
Productivity growth (intermediate)	g_{A_Z}	0.021	Grid search
Productivity growth (energy)	g_{A_E}	0.001	Grid search, bounded below
Decreasing returns in fertility	ψ	0.30	Grid search
Elasticity of substitution	s	0.90	Grid search, bounded above

5.1 External Calibration

We set the pure rate of time preference ρ equal to 0.01, in line with the expert survey of Drupp et al. (2018), in which the mean recommendation for the rate of pure time preference is 1.1 percent (median 0.5 percent). As a check on this choice, the benchmark calibration then implies a savings rate of about one third, comparable to the world average gross saving rate.

We take the parameter value for the intergenerational inequality aversion η from the same survey and set it equal to the mean recommendation of 1.35.

Following Adhami et al. (2023), we require the utility function to reproduce their estimate of the value of a year of life in the United States in 2006 of 4.87 years' worth of per-capita consumption. Solving this condition at 2006 US data for consumption, leisure, and fertility yields $\bar{u}$ as a closed-form function of the preference parameters; see Section C.1 for the derivation. At the benchmark calibration the condition implies $\bar{u} = 12.8$. Note that $\bar{u}$ leaves the average utilitarian model entirely unaffected: for $\theta = 0$ it is an additive constant in the objective and drops out of every optimality condition. It matters only for the total utilitarian planner, for whom it measures the per-person value of existence and ensures that the planner values population correctly even when the remaining utility term is negative (Bressler, 2021, Supplementary Material pp.17-19).

We allow for a depreciation rate δ of the capital stock equal to 0.1. The labor share in the intermediate sector, α, and the energy share, b, are standard values in the literature and represent roughly the empirical labor and energy share. The labor share in the energy sector is set to the same value, $\nu = \alpha = 0.6$, as a symmetry assumption between the two sectors.

Mortality We calibrate the demographic dynamics externally using historical data from the World Population Prospects (United Nations, 2022). Mortality is modeled to closely match historical data and official United Nations projections until 2100, while allowing for alternative long-run demographic scenarios thereafter.

Using historical and projected death rates from the World Population Prospects, we estimate the following non-linear specification for the baseline mortality path:

$$d_{\text{base}}(t) = d_0 e^{-g_d t} + \frac{d_{\text{UN}}}{1 + \exp\big[-m_1 (t - t_1)\big]}. \tag{55}$$

The first term captures the exponential decline in mortality since 1960 at rate g_d, reflecting improvements in health, nutrition, and medical technology. The second term introduces a logistic demographic transition component. Here, d_{UN} determines the level implied by UN projections around 2100, m_1 governs the steepness of the transition, and t_1 its midpoint.

This specification reproduces the observed historical mortality decline, but also the UN projected increase in mortality due to population aging resulting in a compositional shift in the population: A relatively bigger share of the population falls into a higher age bin with higher mortality rates. This effect increases overall mortality and works against the decreasing mortality effect of medical advancements. To acknowledge the increasingly scarce and uncertain official projections beyond 2100 (Raftery & Ševčíková, 2023), we construct alternative long-run demographic scenarios using a smooth double-logistic transition that gradually redirects the mortality path toward a scenario-specific lower bound $\bar{d}$:

$$d(t) = d_{\text{base}}(t) - \frac{d_{\text{UN}} - \bar{d}}{1 + \exp\big[-m_2\,(t - t_2)\big]}. \tag{56}$$

This specification smoothly transitions toward the long-run scenario rate $\bar{d}$ via a second logistic correction centered at $t_2 = 200$ with steepness $m_2 = 0.05$.

The parameter $\bar{d}$ determines the long-run mortality floor. We treat $\bar{d}$ as an explicit scenario choice and label each scenario by the population future it induces. The baseline calibration sets $\bar{d} = 0.008$, under which population remains near its peak of around ten and a half billion for the following three centuries. The sensitivity analysis in Section D.3 considers $\bar{d} = 0.007$, under which population keeps rising over the simulated horizon, and $\bar{d} = d_{\text{UN}} = 0.0125$, under which mortality simply stays at its projected 2100 level and population declines visibly. The three scenarios induce qualitatively different long runs, and we report which case of the analytical results of Section 4 each of them selects. See Section C.2 for further details.

Fertility and Child-Rearing Costs. Fertility is determined by

$$n(t) = \kappa(t) L_n(t)^{\psi}, \tag{57}$$

where $\psi \in (0, 1]$ captures decreasing returns in child-rearing time and $\kappa(t)$ governs the time cost of raising children.

Using UN data on global fertility and time allocation until 2100, we estimate the time path of child-rearing costs from

$$\frac{n(t)}{\bar{L}_n^{\psi}} = \kappa(t) = \kappa_0 e^{-g_\kappa t} + \bar{\kappa}. \tag{58}$$

Thus, fertility declines over time due to the gradual increase in the effective time cost of raising children, converging toward a long-run level $\bar{\kappa}$. The parameter κ_0 captures the initial child-rearing cost in 1960, while g_κ governs the speed of adjustment. We evaluated data from the American time use survey from the US Bureau of Labor Statistics processed by Our World in Data and calculate that an average American spends roughly 12.46% of her life time with children (OurWorldinData, 2023). So that roughly $\bar{L}_n = 0.125$, which is also in line with the equilibrium time spent rearing children in Jones (2022a). The estimation holds $\bar{L}_n$ fixed at this value, so the fitted path $\kappa(t)$ reproduces observed fertility for allocations near this level of child-rearing time.

Importantly, the calibration of $(\kappa_0, \bar{\kappa}, g_\kappa)$ is conditional on the degree of decreasing returns ψ. For each value of ψ, we estimate a non-linear regression in R and obtain a corresponding parameter triplet. This procedure ensures that the model reproduces the observed fertility transition for a wide range of ψ values. The resulting estimates are reported in Section C.2.

The initial population level is set to $P_0 = 3$ corresponding to the world population (in billions) in 1960 (United Nations, 2022).

Energy The analytical production function uses energy in model units, where one model unit corresponds to ϕ_E exajoules (EJ) of physical energy. The scaling parameter ϕ_E converts between the two and is calibrated to match the observed energy intensity in 1960,

$$\phi_E = \frac{E_{1960}}{Y_{1960}} = \frac{145.75 \text{ EJ}}{10.88 \text{ trln USD}} \approx 13.4. \tag{59}$$

Finally, the upper bound on renewable energy inflow is set to $\bar{E} = 10{,}000$ EJ. This value is motivated by estimates of the global technical potential of solar energy. Technical potential refers to the amount of energy that could be generated with current (or near-commercial) technologies after accounting for geographical availability, land-use restrictions, spacing requirements, conversion efficiencies, and other engineering

constraints, while abstracting from economic, institutional, or social feasibility considerations. The comprehensive review by Angliviel De La Beaumelle et al. (2023) reports that global solar technical potential (utility-scale PV, rooftop PV, and CSP combined) spans a wide range, from roughly 400 EJ/year at the lower bound to about 86,000 EJ/year at the upper bound. Central estimates are substantially smaller: the median across studies is approximately 7,500 EJ/year and the mean around 15,000 EJ/year. Setting $\bar{E} = 10{,}000$ EJ therefore anchors the calibration within the central range of estimates reported in the literature. In comparison, current global energy consumption is in the range of 600 EJ. In the sensitivity analysis presented in Section D.1, we vary this parameter and show that changes in $\bar{E}$ affect primarily the timing at which the constraint becomes binding. The underlying mechanisms and qualitative results of the model, however, remain unaffected.

5.2 Internal Calibration

Boppart and Ngai (2021) construct a time series on the leisure share based on US time survey data for 1965-2013. They find that the leisure share slowly increases from 0.35 in 1965 to 0.42 in 2013, but that there is huge heterogeneity between different education groups. We calibrate the leisure parameter γ so that the model's leisure share in 2006 equals the value of 0.396 in the US time use data. This yields $\gamma = 0.818$.

Initial values for the capital stock and productivity $(K_{Z,0}, K_{E,0}, A_{Z,0}, A_{E,0})$ are chosen to match the output and energy consumption level in 1960, together with a capital-output ratio of 2.3 and an energy share of the capital stock of ten percent.

Grid Search We calibrate the remaining parameters $(\psi, g_{A_Z}, g_{A_E}, s)$ by matching the social planner's solution to observed aggregate trends. We perform a sequential grid search to identify the parameter combination that minimizes the discrepancy between the simulated trajectories of the model and the empirical data on population, fertility, energy intensity, and output per capita between 1960 and 2020. The preference for children is identified through the composite $\epsilon\psi$, which governs the share of time devoted to child-rearing in the planner's time-allocation condition. Thus, we normalize $\epsilon = 1$ and only calibrate ψ in the grid search process.

The search proceeds in the order ψ (fertility curvature), g_{A_Z} (GDP per capita growth), and $g_{A_E} \times s$ (energy intensity level and trend), each stage conditioning on the current values of the others. Because such a sequential search can depend on where it

starts, we run it from twelve starting points that span the admissible parameter ranges, and iterate each run twice. All twelve runs converge to the same parameter region. To guard against spurious local solver optima, neighboring grid points are solved with warm starts along the grid, and every candidate combination is ranked at its best available solution. Section C.3 reports the grid ranges and the procedure in detail.

For each parameter tuple, the model is solved in Julia using the Ipopt algorithm. The resulting time series are merged with the empirical data and the fit is evaluated by the sum of squared log deviations between model outcome and empirical data for four key variables: Population (P), Fertility (n), GDP per Capita (Y/P), and Energy Intensity (E/Y). The parameter combination yielding the smallest total deviation is selected as the internally calibrated benchmark.

Figure 1 shows our baseline calibration versus the empirical time series for our four matched variables and two unmatched variables: GDP (Y) and Energy (E).

The best-fitting parameter combination among the tuples evaluated yields a total loss of $L = 0.0672$. Since the loss function is defined as the sum of squared log deviations between model outcome and empirical data across all variables and time periods, dividing by the total number of observations provides the mean squared log deviation. With 28 matched data points (four variables over seven decades), the mean squared log deviation equals $0.0672/28 = 0.0024$, implying a root-mean-square log deviation of $\sqrt{0.0024} \approx 0.049$. Hence, the calibrated model reproduces the historical dynamics of population, fertility, energy intensity, and output per capita with a root-mean-square deviation of about 5 percent.

Two parameter values stand out: $s = 0.9$ and $g_{A_E} = 0.001$. First, the elasticity of substitution is high because the model has no channel for improving energy efficiency in final use. Historically, much of the decline in energy intensity came from converting primary energy into useful services more efficiently, with global average conversion efficiency reaching roughly eleven percent by 2005 (Cullen & Allwood, 2010). Our model captures this trend by substituting away from energy, which biases s upward. Since efficiency gains are bounded by the thermodynamic minimum of each energy service, the estimated s is best read as an upper bound on long-run future substitutability. Second, the unconstrained grid search drives energy-sector productivity growth to zero. Over the calibration period energy is almost entirely fossil, and extracting it did not become cheaper in terms of labor and capital: technological progress in extraction was offset by depletion. To capture the ongoing transition to renewables and the productivity

gains it brings, we set g_{A_E} to the smallest positive value on the grid, 0.001.

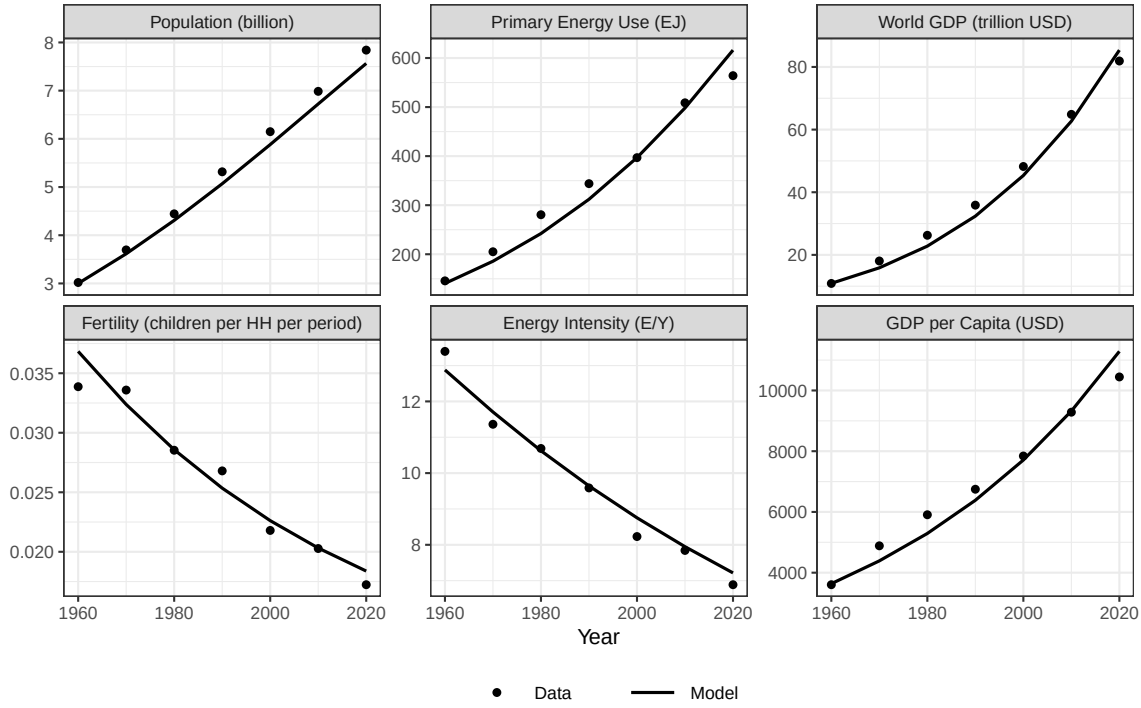


Figure 1: Data vs. Model. Population Data from United Nations (2022); Energy data from bp (2022) and Smil (2017); GDP data from Bolt and van Zanden (2020).

6 Numerical Results

The model is implemented as a JuMP model in Julia and solved utilizing the Ipopt solver algorithm. All runs are solved on ten-year steps through the year 2750, while figures display the paths up to 2500, leaving a buffer against terminal-horizon effects. We present numerical results for the average utilitarian case ($\theta = 0$) mimicking a decentralized economy in which a dynastic household receives utility from having children but does not receive utility from the size of the dynasty. We then discuss two extensions of the model as a thought experiment. First, the case of a total utilitarian social planner ($\theta > 0$) and, second, the case of endogenous growth. We examine the sensitivity of our results with respect to the energy limit, $\bar{E}$ (Section D.1), the elasticity of substitution, s (Section D.2) and the long-run mortality rate, $\bar{d}$ (Section D.3).

6.1 Average Utilitarian Planner

Emergence of the Leisure Economy Figure 2 reports the baseline simulation for the average utilitarian benchmark ($\theta = 0$) from 1960 to 2500 under two scenarios: a baseline run without an energy cap (solid line) and a run with a binding energy limit (dashed line). The figure plots aggregate output $Y(t)$, energy use $E(t)$, total and per-capita consumption $C(t)$ and $c(t)$, the capital stock $K(t)$, TFP in the energy sector $A_E(t)$, the allocation of time between work $L_Z(t) + L_E(t)$ and leisure $l(t)$, and the scarcity rent $q(t)$.

The dynamics are characterized by two distinct phases. In the first phase, the economy behaves like a standard neoclassical growth model. The resource constraint is not binding and productivity growth translates into rising aggregate quantities: output, consumption, and the capital stock grow at the rate implied by technological progress. The time allocation is nearly stationary: the planner keeps work and leisure shares approximately constant. The King–Plosser–Rebelo preference structure cancels out income and substitution effects along a balanced-growth path. There is almost no difference between an economy with and without energy limit.

The second phase begins when energy use hits the upper bound and the constraint becomes binding, $E(t) = \bar{E}$, indicated by the dotted vertical line. From that point onward, additional labor-augmenting productivity can no longer be converted into proportionate increases in material output because energy, as an essential input with limited substitutability ($s < 1$), constrains output and consumption growth. Aggregate output and total consumption grow less and ultimately converge to a constant level determined by $\bar{E}$.[4] Continued productivity growth instead relaxes the input requirement for producing final output. The social planner adjusts production by lowering labor input. Consequently, work time declines whereas leisure increases.

A final implication of the binding constraint is the emergence and growth of a scarcity rent. When $E(t) = \bar{E}$, energy is no longer a freely expandable intermediate input, and its shadow value increases.

The post-cap phase is a transition from growth in quantities to growth in leisure time. Innovation continues, but its welfare payoff is realized through reduced labor and capital requirements rather than higher material consumption.

[4]Since in our baseline calibration the elasticity of substitution is relatively high ($s = 0.90$) the upper bound on GDP is large and not reached within the displayed time horizon of the next 500 years. See the long-run paragraph at the end of this subsection.

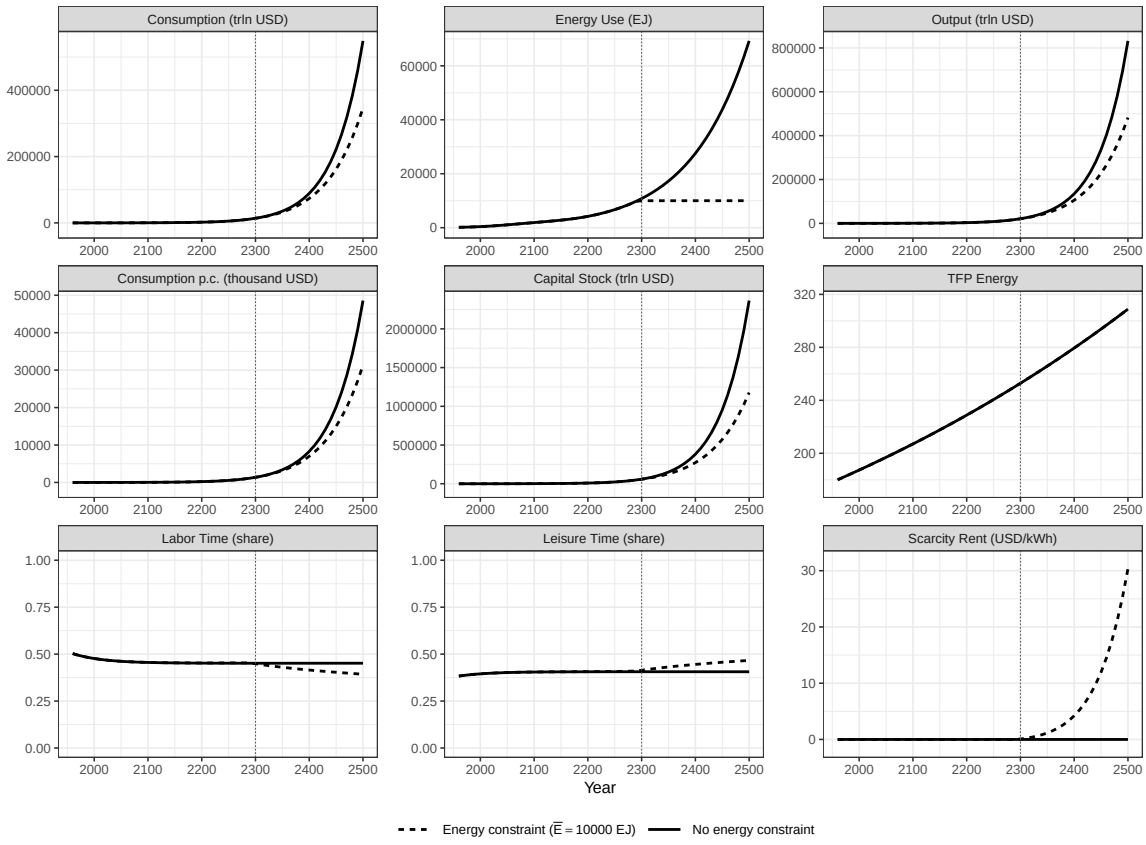


Figure 2: Evolution of different variables. Average Utilitarian ($\theta = 0$).

Baumol's Energy Cost Disease Figure 3 plots the income shares accruing to labor, capital, and the scarcity rent. The scarcity rent is equal to zero in the no-limit economy as well as the corresponding income share. Moreover, along the simulated balanced-growth path the labor and capital shares are constant at 60% and 40%, reflecting stable input cost shares in the two Cobb-Douglas sub-technologies.

Once the limit becomes binding, the decomposition of the energy share in Equation (34) implies a sharp qualitative change. Because energy is essential and imperfectly substitutable ($s < 1$), the expenditure share of energy in final output rises over time. At the same time, continued productivity growth reduces the amounts of capital and labor required to harvest the fixed energy flow, so that the wage and capital-income components of the energy share shrink.

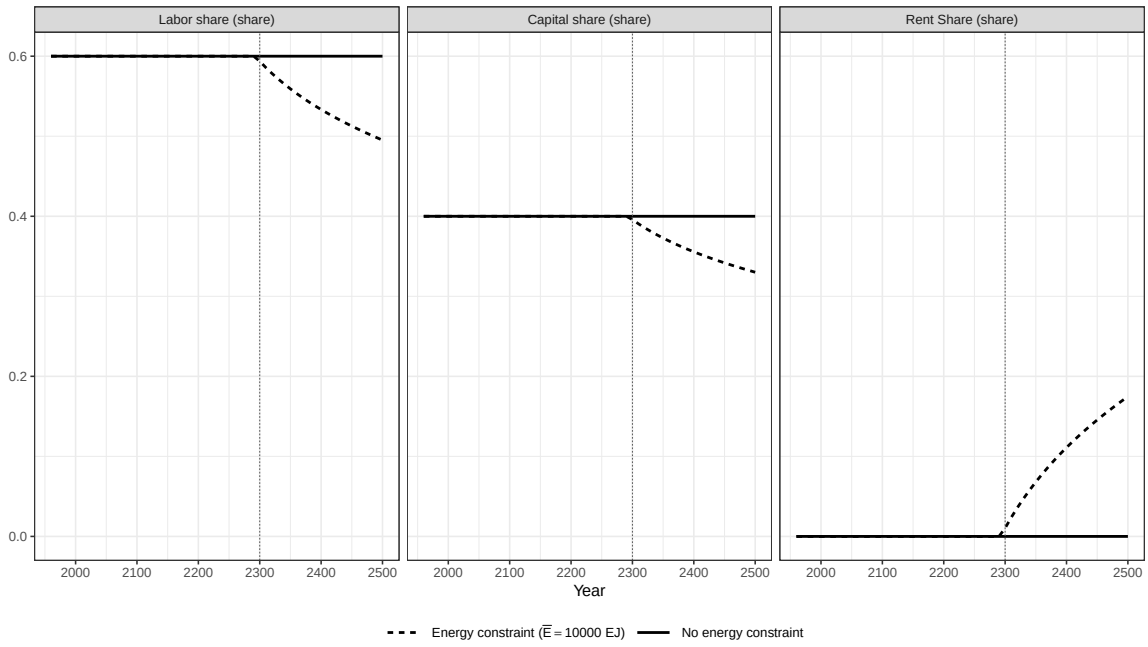


Figure 3: Factor Shares. Average Utilitarian ($\theta = 0$).

This pattern mirrors Baumol's original cost disease (Baumol, 1967), but with an essential renewable resource sector replacing Baumol's stagnant service sector. However, scarcity rather than low productivity growth drives the increasing share associated with the constrained input. In our setting, the wedge is a textbook scarcity rent and thus conceptually distinct from returns to reproducible capital or labor effort. In principle, such rents can be taxed with low efficiency costs, which suggests scope for redistribution in the phase where the economy transitions toward higher leisure.

Since we think in our framework about solar energy and thus, solar panels covering land surface, this redistribution argument closely parallels Henry George's classic case for a land value tax. George (1879/1935) emphasizes that the rental value of land reflects scarcity and location advantages rather than productive effort. As a result, taxing land rent can finance public purposes without discouraging labor supply or capital formation. The scarcity rent in our model plays the same conceptual role. Once the energy flow is capped at $\bar{E}$, the term $q(t)\bar{E}$ is a payment for access to a fixed natural input. Unlike taxes on wages or on the return to reproducible capital, a levy on this rent does not distort the margin of producing additional energy nor does it directly penalize effort or accumulation elsewhere in the economy. In this sense, the transition to an energy-constrained steady state generates an increasingly large tax base that could, in principle, support redistribution with comparatively low efficiency costs.

Population Dynamics Figure 4 reports time rearing children $L_n(t)$, fertility $n(t)$, and population $P(t)$. In the no-limit economy, the planner gradually increases time spent on child rearing and eventually stabilizes $L_n(t)$ at a high level. Because child production exhibits diminishing returns and the calibrated cost shifter $\kappa(t)$ declines over time, fertility falls even as $L_n(t)$ rises.

With a binding energy constraint in the future, fertility choices adjust already in the unconstrained phase. In particular, $L_n(t)$ is below the no-limit benchmark even before the limit is binding. The average utilitarian social planner anticipates that once $E(t) = \bar{E}$ binds, aggregate output grows less and in the limit stagnates. Thus, population growth ultimately reduces per-capita consumption: a trade-off the planner foresees. Anticipation operates through the shadow values of the economy's stocks. Solving eq. (19) forward expresses the current shadow value of an additional person as a discounted integral over the entire future path (see eq. (77)). Once this future contains an energy limit, the return to fertility is already lowered today. Discounting implies that this gap widens over time as the binding date approaches. The same forward-looking logic also applies to the co-state of the energy capital stock.

The Long Run Every path in Figures 2 to 4 shows transitional dynamics: the limit statements of Section 4.3 lie beyond the displayed horizon. Once the cap binds permanently, Lemma 1 pins down where the economy is heading to in the long-run: output and consumption converge to the bound $\bar{Y} = b^{1/\sigma}\bar{E}$, work time vanishes, and the

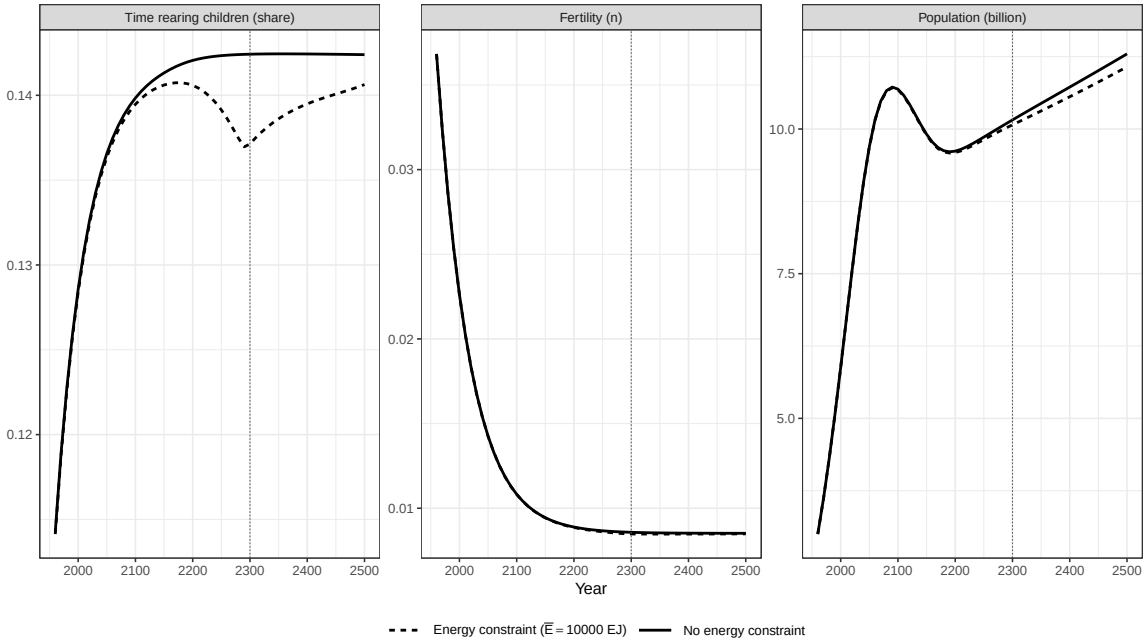


Figure 4: Population Dynamics. Average Utilitarian ($\theta = 0$).

scarcity rent absorbs the entire energy share, the price of energy approaching $\bar{q} = b^{1/\sigma}$. How distant these limits are is governed by the substitution elasticity. Table 5 reports the output bound across s and $\bar{E}$: at $s = 0.5$ and the baseline cap of 10,000 EJ, world GDP could still expand roughly 75-fold from today's level. At the calibrated $s = 0.90$ the bound is astronomical, which is why output keeps growing in Figure 2 centuries after the cap binds. Evaluating the replacement value in eq. (53) for our baseline calibration gives $R = 0.81 < 1$: the planner does not sustain a stationary population. Fertility settles at the fixed point of eq. (54), implying a settled population decline of 0.06 percent per year, and since $g_{A_E} + \hat{g}_P > 0$, the effective energy workforce keeps growing: the cap remains binding forever and the full leisure economy emerges: future (ii), the leisure economy on an empty planet. None of this is visible in the figures. The mortality path settles only around 2300 and convergence to the settled decline has a half-life of roughly a millennium, which is why displayed population still drifts upward while it will fall in the long run. The mortality scenarios in Section D.3 select the other two futures; the following two subsections instead vary the welfare criterion and the growth engine.

Table 5: Long-run output $\bar{Y}$ (trillion USD) with $b = 0.1$.

	Elasticity of substitution s			
$\bar{E}$ (EJ)	0.3	0.5	0.7	0.9
5,000	1,001	3,731	80,376	$3.7 \cdot 10^{11}$
10,000	2,002	7,463	160,752	$7.5 \cdot 10^{11}$
20,000	4,004	14,925	321,505	$1.5 \cdot 10^{12}$

6.2 Total Utilitarian Planner

The results so far rest on average utilitarian welfare. As a thought experiment, we now ask how the optimal path changes if society adopted total utilitarian preferences from today onward. History up to 2020 is given by the baseline model, which fits the data. From 2020 on, the planner maximizes welfare with $\theta = 1$, starting from the baseline model's 2020 state, with all parameters at their baseline calibrated values. Trajectories therefore coincide until 2020 and differ afterwards depending only on the welfare criterion. Each scenario (with and without energy constraint) starts from the 2020 state of the corresponding baseline scenario. Figure 5 reports the results.

The switch is drastic. The total utilitarian planner raises time devoted to child rearing from about 13% to roughly 70% of the time endowment, and this share approaches 90% by 2500, while leisure and market work collapse. As a result population explodes with and without the energy cap, exceeding 200 billion by 2500. Under total utilitarianism the planner prioritizes population over per-capita consumption, which ends up an order of magnitude below its average-utilitarian level. The qualitative finding of Baumol's Energy Cost Disease survives: once the cap binds – which happens two decades earlier than in the baseline, since a larger population is pressing against it – the scarcity rent emerges and follows the same path as in the average utilitarian economy.

The two welfare criteria adjust to the energy cap on different margins. The average utilitarian pre-adjusts population and leaves hours essentially untouched before the cap binds. The total utilitarian decreases market work rapidly in favor of child rearing time, but only slightly in response to the limit leading to only small increases in leisure time. Child-rearing time is almost untouched. The reason lies in the composition of the forward-looking return to fertility in eq. (19): for $\theta = 1$ the value of a person is dominated by the value-of-life term $\theta U/U_c$, which the cap cannot devalue. A

capped economy still delivers $\bar{u}$ per person-year. The population margin is thus nearly insensitive to the constraint.

As in the average utilitarian case, the figures show only the transition – the long run, however, now differs sharply. By part 1(b) of Proposition 1, a total utilitarian planner sustains a stationary population for every R: the total utilitarian never chooses the empty planet. Instead of future (ii), the economy heads for future (i): the full leisure economy with a stationary population. In the limit the two criteria diverge completely: average utilitarianism yields a slowly emptying planet of ever-richer people, total utilitarianism a vast population at low consumption per capita.

6.3 Endogenous Growth

The results so far treat productivity growth as exogenous. Both Baumol's energy cost disease and the leisure economy hinge on the growth rate of the effective energy workforce, $G = g_{A_E} + g_P$. Population growth has been endogenous throughout. As a second thought experiment, we now also endogenize the other component, productivity growth. As with total utilitarianism, the planner solution is not a positive description of history. Here the reason is that ideas are nonrival: the planner internalizes the full social return to research and devotes far more time to R&D than observed in the data. We therefore proceed as in Section 6.2 and treat history up to 2020 as the exogenous baseline, which fits the data. From 2020 on the planner additionally chooses research time in both sectors, starting from the baseline model's 2020 state. The full model and calibration are presented in Section E.

We assume a semi-endogenous growth process in which productivity in sector $i \in \{Z, E\}$ evolves according to

$$\dot{A}_i(t) = \zeta_i \big(L_{R,i}(t) P(t)\big)^{\omega} A_i(t)^{1-\beta_i}. \tag{60}$$

Research time $L_{R,i}(t)$ now also enters the time constraint eq. (8) alongside work, child rearing, and leisure. The parameter $\beta_i > 0$ captures the rate at which ideas become harder to find, ω captures duplication among researchers, and ζ_i scales research productivity (Bloom et al., 2020; Jones, 1995). With $\beta_i > 0$, sustaining exponential growth requires ever-growing research effort. Research time, however, is bounded between zero and one and population cannot rise indefinitely, while the return to research erodes as knowledge accumulates through $A_i(t)^{1-\beta_i}$: productivity growth must eventually fade

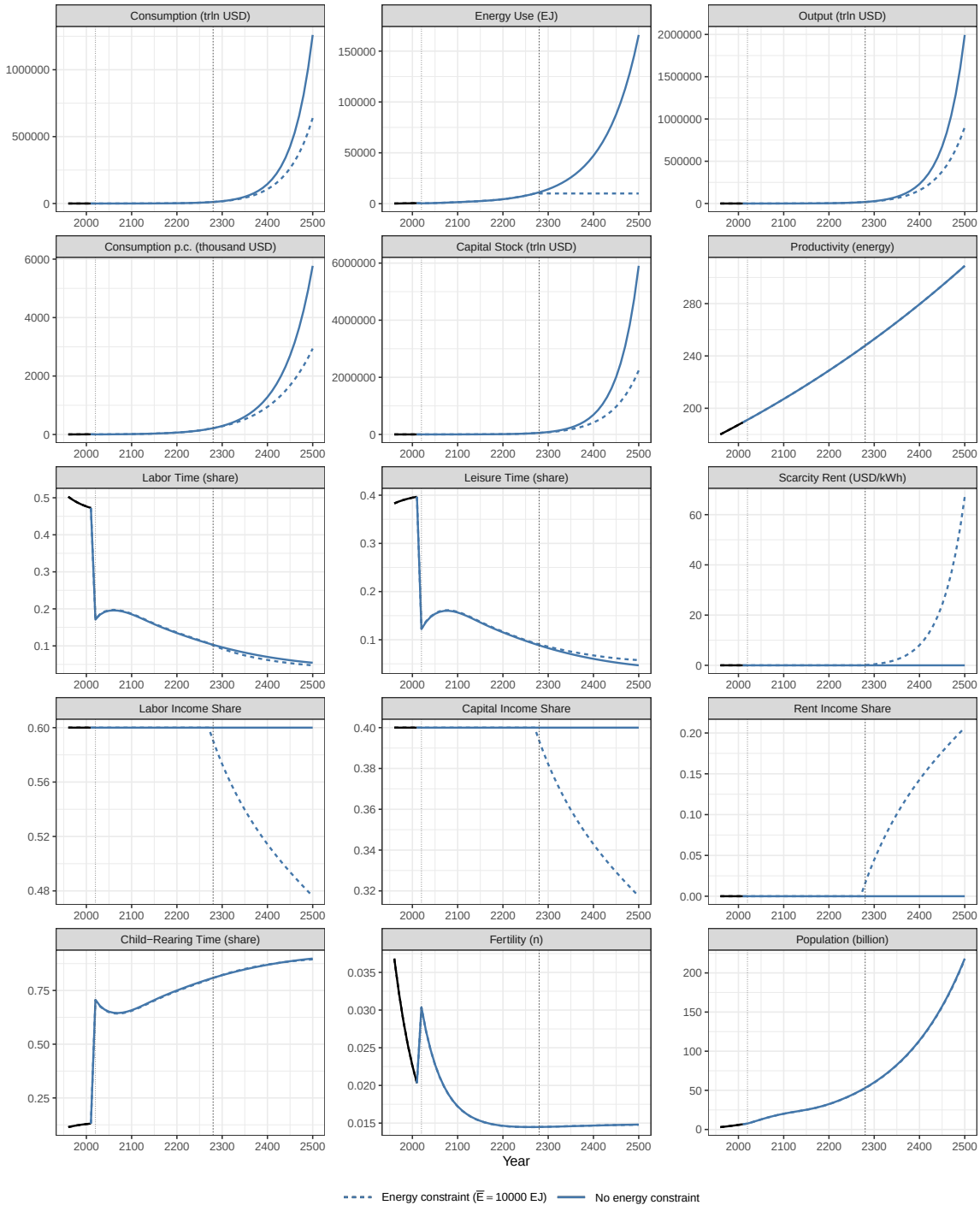


Figure 5: Results for the Total Utilitarian Planner from 2020 onward ($\theta = 1$). Black lines denote historical values; blue lines the model outcomes.

(Jones, 2022a). We present two possible futures differing only in the idea depletion parameter β_E. Either energy, and with it output, runs into the physical cap $\bar{E}$ (energy-bound future), or growth fades before the cap is reached because ideas become too hard to find (idea-bound future). We set the duplication value, common to both sectors, equal to $\omega = 0.5$, which is roughly the level Fort et al. (2026) find on the firm level in more recent years. Idea-depletion in the intermediate sector is set equal to $\beta_Z = 1.5$, which is in line with the estimates in Bloom et al. (2020) and Jones (2022b) for $\omega = 0.5$. ζ_i is a scale parameter, normalized so that the technology delivers the observed 2020 growth rates at the observed 2020 research inputs (see Section E).

The energy-bound future ($\beta_E = 0.2$). When energy ideas run out slowly, energy-augmenting productivity rises strongly, increasing output and energy use. The green lines in Figure 6 contrast the constrained and unconstrained paths of this energy-bound future. In the model run with the energy limit (dashed green), the cap is reached in 2330 and we see the same effects as in the baseline model: consumption, output and the capital stock diverge, a scarcity rent emerges, and work-time and child-rearing time are reduced in favor of increasing leisure time. Additionally, research time in the energy sector is now also reduced, which happens even before the cap becomes binding. This is the same anticipation mechanism as discussed in Section 6.1 for population. Once energy is fixed at the cap, better energy technology no longer expands output but only lowers the labor and capital needed to harvest the fixed flow, so the planner's incentive to fund energy research falls.[5] Moreover, higher levels of TFP are only desirable from the planner's perspective as long as the marginal benefit from one more unit of research exceeds the marginal benefit of one more unit of leisure. With decreasing returns to research, one hour of research will eventually free up only one hour of work time — an hour that could have been worked directly in the first place.

The idea-bound future ($\beta_E = 1.5$). When energy ideas run out as fast as ideas for the intermediate good, the energy limit is not reached within the simulated horizon. The orange line in Figure 6 shows that energy-augmenting productivity grows more slowly and energy demand stays below the cap. Here the constrained and unconstrained

[5] This is contrary to the idea of price-driven resource scarcity stimulating energy-saving innovation and resource expansion (Hassler et al., 2021). However, since in our model setup the resource cannot be expanded and already operates at the thermodynamically optimal level, further research cannot circumvent the limit.

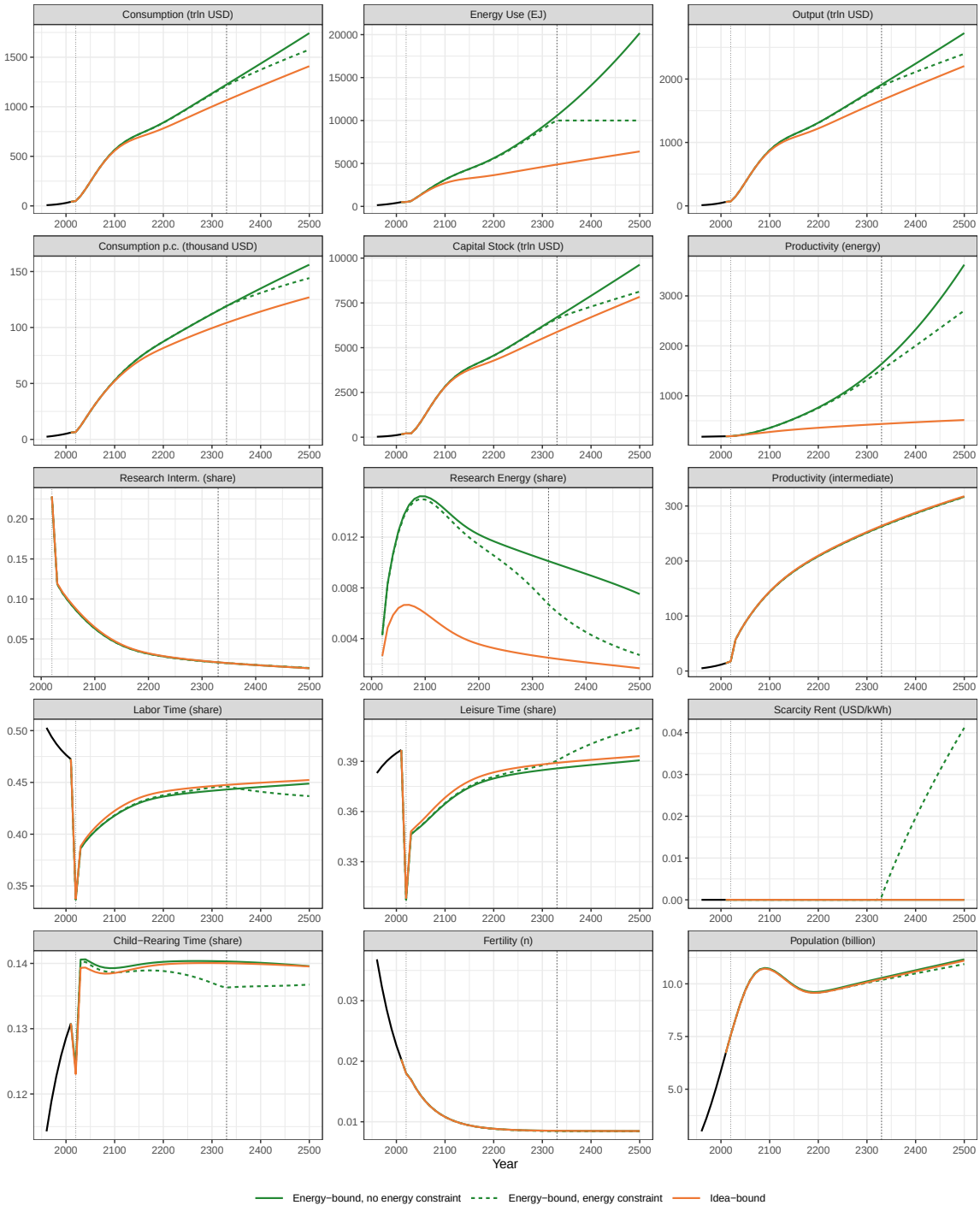


Figure 6: Results for Endogenous Growth: Green, the energy-bound future ($\beta_E = 0.2$) and Orange, the idea-bound future ($\beta_E = 1.5$). Black lines denote historical values.

paths are indistinguishable throughout. No scarcity rent appears, and growth fades out through idea depletion rather than hitting the energy cap.

7 Conclusion

This paper studies an economy in which material output eventually becomes bounded by an essential but finite renewable input, while labor-augmenting innovation continues. We develop a modified Ramsey framework with endogenous time allocation and endogenous population to ask where productivity gains go when output is bounded.

We find that, once the limit becomes binding, a growing scarcity rent erodes the labor share, and productivity gains go to leisure. Without the limit, work time would stay almost constant. The numerical simulations calibrated to the global economy illustrate this transition over the coming centuries. For a binding cap and continued productivity growth, the constrained economy departs from its unconstrained counterpart: output, consumption, and the capital stock grow more slowly, work time falls, and leisure increases steadily. In the spirit of Keynes (1930), technological progress leads to work-time reduction and ultimately to a materially bounded leisure economy. At the calibrated parameters the economy approaches an empty-planet leisure economy in the long run. Population eventually declines while the cap remains binding and leisure absorbs the freed time.

Since energy is essential, only imperfectly substitutable and in limited supply, its share in total spending rises once the cap binds. We refer to this phenomenon as Baumol's Energy Cost Disease. In contrast to the original Baumol's Cost Disease (Baumol & Bowen, 1966), the resulting scarcity rent in our model might be taxed efficiently without any distortions and redistributed at will. This contrasts with other visions of zero-growth or post-growth economies in which the distributional question is at the core and it is often argued that redistribution in a zero-growth world becomes more complicated. We want to emphasize that this vision relies on strong democratic institutions that prioritize the well-being of their citizens. The same model framework could also describe a scenario where an energy monopolist captures scarcity rents, leading to widespread unemployment and limited access to leisure for the majority of the population. The key distinction lies in the resource distribution at the individual level. Therefore, the presence of a robust democratic state capable of efficiently taxing and redistributing scarcity rents is crucial to ensure equitable outcomes.

A binding limit also influences the population dynamic. The prospect of a future binding energy constraint lowers the shadow value of fertility already in the unconstrained phase. The social planner reduces the time spent rearing children relative to a no-cap counterfactual because additional population growth implies stronger reductions in per-capita consumption once output is bounded. This anticipation channel generates lower fertility and a smaller population path well before the cap binds.

Switching the objective to a total utilitarian planner from 2020 onwards redirects time massively toward child rearing and puts population on a path an order of magnitude above the baseline, with or without the energy constraint. The constraint no longer disciplines population at all: the value of an additional life is dominated by the utility constant and nearly unaffected by the cap.

Endogenizing the growth process makes hitting the energy constraint itself endogenous. If energy ideas deplete slowly, energy use grows into the cap and the main mechanisms stay untouched. Research is pursued up until the marginal benefit of technological progress is equal to the marginal benefit of additional leisure. If energy ideas run out first, energy demand remains below the cap and the constraint does not bind within the simulated horizon. Growth fades out by idea depletion, with no rent and no cost disease. This shows that productivity gains are the precondition of the leisure economy, since without new ideas neither output nor leisure can grow.

Future research could investigate the distributional implications of a binding resource constraint, in particular optimal redistribution of the scarcity rent. Furthermore, the demographic side of the model is stylized. Fertility and mortality are cohort-specific, and while both declined over past decades, the crude death rate will rise as the global population ages. Since environmental pressure, resource scarcity, and innovation all scale with population, gaining a better understanding of how demographic variables respond to and shape economic outcomes is crucial for studying the long-run perspective of humanity.

Finally, our baseline model describes a world in which artificial intelligence generates new ideas without human time input. If this becomes reality, ideas will not be a constraining factor, energy and environmental limits will and the income of this weak link then accrues as a scarcity rent rather than as labor or capital income. The economy we describe – a rising scarcity rent, shrinking work time, and fertility that adjusts in anticipation of the limit – is a picture of what such a future might look like.

Funding Statement

Tobias Bergmann acknowledges a doctoral scholarship from the Heinrich Böll Stiftung and funding from the Bundesministerium für Forschung, Technologie und Raumfahrt (BMFTR) under the ARIADNE project (grant 03SFK5J0). The funders had no role in study design, data collection and analysis, decision to publish, or preparation of the manuscript.

References

Adhami, M., Bils, M., Jones, C. I., & Klenow, P. J. (2023). Population and Welfare: The Greatest Good for the Greatest Number. *National Bureau of Economic Research Working Paper Series, No. 31999*. https://doi.org/10.3386/w31999

Aghion, P., Jones, B. F., & Jones, C. I. (2017). Artificial Intelligence and Economic Growth. *NBER Working Paper Series, Working Paper 23928*. https://doi.org/10.3386/w23928

Angliviel De La Beaumelle, N., Blok, K., De Chalendar, J. A., Clarke, L., Hahmann, A. N., Huster, J., Nemet, G. F., Suri, D., Wild, T. B., & Azevedo, I. M. (2023). The Global Technical, Economic, and Feasible Potential of Renewable Electricity. *Annual Review of Environment and Resources*, *48*(1), 419–449. https://doi.org/10.1146/annurev-environ-112321-091140

Baumol, W. J. (1967). Macroeconomics of Unbalanced Growth: The Anatomy of Urban Crisis. *The American Economic Review*, *57*(3), 415–426.

Baumol, W. J., & Bowen, W. G. (1966). *Performing Arts, The Economic Dilemma: A study of problems common to theater, opera, music, and dance.* Cambridge, Mass.: M.I.T. Press.

Baumol, W. J., & De Ferranti, D. M. (2012). *The cost disease: Why computers get cheaper and health care doesn't*. Yale University Press.

Bayer, C., Kriwoluzky, A., Müller, G. J., & Seyrich, F. (2023). Hicks in HANK: Fiscal Responses to an Energy Shock. *SSRN Electronic Journal*. https://doi.org/10.2139/ssrn.4619906

Bergmann, T., & Kalkuhl, M. (2025). Decoupling economic growth from energy use: The role of energy intensity in an endogenous growth model. *Ecological Economics*, *230*, 108519. https://doi.org/10.1016/j.ecolecon.2025.108519

Bilancini, E., & D'Alessandro, S. (2012). Long-run welfare under externalities in consumption, leisure, and production: A case for happy degrowth vs. unhappy growth. *Ecological Economics*, *84*, 194–205. https://doi.org/10.1016/j.ecolecon.2011.10.023

Bloom, N., Jones, C. I., Van Reenen, J., & Webb, M. (2020). Are Ideas Getting Harder to Find? *American Economic Review*, *110*(4), 41.

Bolt, J., & van Zanden, J. L. (2020). Maddison Project Database, version 2020. *Maddison style estimates of the evolution of the world economy. A new 2020 update.*

Boppart, T., & Ngai, L. R. (2021). Rising inequality and trends in leisure. *Journal of Economic Growth*, *26*(2), 153–185. https://doi.org/10.1007/s10887-021-09189-8

bp. (2022). *Bp - Statistical Review of World Energy 2022*. bp. http://www.bp.com/statisticalreview

Brander, J. A., & Taylor, M. S. (1998). The Simple Economics of Easter Island: A Ricardo-Malthus Model of Renewable Resource Use. *The American Economic Review*, *88*(1), 119–138. http://www.jstor.org/stable/116821

Bressler, R. D. (2021). The mortality cost of carbon. *Nature Communications*, *12*(1), 4467. https://doi.org/10.1038/s41467-021-24487-w

Bretschger, L. (2020). Malthus in the light of climate change. *European Economic Review*, *127*, 103477. https://doi.org/10.1016/j.euroecorev.2020.103477

Bretschger, L., & Jo, A. (2024). Complementarity between labor and energy: A firm-level analysis. *Journal of Environmental Economics and Management*, *124*, 102934. https://doi.org/10.1016/j.jeem.2024.102934

Burda, M., & Zessner-Spitzenberg, L. (2024). Greenhouse Gas Mitigation and Price-Driven Growth in a Solow-Swan Economy with an Environmental Limit. *SSRN Electronic Journal*. https://doi.org/10.2139/ssrn.4709704

Bureau of Labor Statistics. (2007). American Time Use Survey - 2006 Results. *News United States Department of Labor*.

Córdoba, J. C., & Liu, X. (2022). Malthusian stagnation is efficient. *Theoretical Economics*, *17*(1), 415–460. https://doi.org/10.3982/TE3542

Cullen, J. M., & Allwood, J. M. (2010). Theoretical efficiency limits for energy conversion devices. *Energy*, *35*(5), 2059–2069. https://doi.org/10.1016/j.energy.2010.01.024

Dasgupta, P. (2021). *The Economics of Biodiversity: The Dasgupta Review*. HM Treasury.

Dasgupta, P., & Heal, G. (1974). The Optimal Depletion of Exhaustible Resources. *The Review of Economic Studies*, *41*, 3–28. https://doi.org/10.2307/2296369

Dasgupta, P., & Heal, G. (1979). *Economic Theory and Exhaustible Resources* (Repr.). Cambridge Univ. Pr.

Dietz, S., & Lanz, B. (2025). Growth and adaptation to climate change in the long run. *European Economic Review*, *173*, 104982. https://doi.org/10.1016/j.euroecorev.2025.104982

Doepke, M., Hannusch, A., Kindermann, F., & Tertilt, M. (2022). The Economics of Fertility: A New Era. *National Bureau of Economic Research Working Paper Series*, *No. 29948*. https://doi.org/10.3386/w29948

Drupp, M. A., Freeman, M. C., Groom, B., & Nesje, F. (2018). Discounting Disentangled. *American Economic Journal: Economic Policy*, *10*(4), 109–134. https://doi.org/10.1257/pol.20160240

Fagnart, J.-F., Germain, M., & Van Der Linden, B. (2023). Working time reduction and employment in a finite world*. *The Scandinavian Journal of Economics*, *125*(1), 170–207. https://doi.org/10.1111/sjoe.12513

Fort, T. C., Goldschlag, N., Liang, J., Schott, P. K., & Zolas, N. (2026). Growth is Getting Harder to Find, Not Ideas. *NBER Working Paper*.

FRED. (2024). *Real personal consumption expenditures per capita* (A794RX0Q048SBEA).

Fried, S. (2018). Climate Policy and Innovation: A Quantitative Macroeconomic Analysis. *American Economic Journal: Macroeconomics*, *10*(1), 90–118. https://doi.org/10.1257/mac.20150289

Fried, S., Novan, K., & Peterman, W. B. (2022). Climate policy transition risk and the macroeconomy. *European Economic Review*, *147*, 104174. https://doi.org/10.1016/j.euroecorev.2022.104174

George, H. (1935). *Progress and Poverty: An Inquiry into the Cause of Industrial Depressions and of Increase of Want with Increase of Wealth: The Remedy* (Fiftieth Anniversary Edition). Robert Schalkenbach Foundation. (Original work published 1879)

Gerlagh, R. (2023). Climate, technology, family size; on the crossroad between two ultimate externalities. *European Economic Review*, *152*, 104376. https://doi.org/10.1016/j.euroecorev.2023.104376

Gerlagh, R., Lupi, V., & Galeotti, M. (2023). Fertility and climate change. *The Scandinavian Journal of Economics*, *125*(1), 208–252. https://doi.org/10.1111/sjoe.12520

Gerlagh, R., & Van Der Zwaan, B. (2002). Long-Term Substitutability between Environmental and Man-Made Goods. *Journal of Environmental Economics and Management*, *44*(2), 329–345. https://doi.org/10.1006/jeem.2001.1205

Hamilton, B. E., Martin, J. A., & Ventura, S. J. (2007). National Vital Statistics Report. *CDC*.

Hassler, J., Krusell, P., & Olovsson, C. (2021). Directed Technical Change as a Response to Natural Resource Scarcity. *Journal of Political Economy*, *129*(11), 3039–3072. https://doi.org/10.1086/715849

Hinkelmann, S. (2024). (Be-)Coming Clean: A Model of the U.S. Energy Transition. *Job Market Paper*. https://drive.google.com/file/d/1YiffYe5vQVDcE58qmANFq3a0E0R-4PfV/view

Jones, C. I. (1995). R & D-Based Models of Economic Growth. *Journal of Political Economy*, *103*(4), 759–784. http://www.jstor.org/stable/2138581

Jones, C. I. (2022a). The End of Economic Growth? Unintended Consequences of a Declining Population. *American Economic Review*, *112*(11), 3489–3527. https://doi.org/10.1257/aer.20201605

Jones, C. I. (2022b). The Past and Future of Economic Growth: A Semi-Endogenous Perspective. *Annual Review of Economics*.

Jones, C. I. (2026). AI and Our Economic Future. *Journal of Economic Perspectives*, *40*(3), 3–22. https://doi.org/10.1257/jep.20261505

Kallis, G., Kalush, M., O.'Flynn, H., Rossiter, J., & Ashford, N. (2013). "Friday off": Reducing Working Hours in Europe. *Sustainability*, *5*(4), 1545–1567. https://doi.org/10.3390/su5041545

Keynes, J. M. (1930). Economic possibilities for our grandchildren, reprinted in John Maynard Keynes, Essays in Persuasion. *New York: W. W. Norton & Co., 1963.*, 358–373.

King, R. G., Plosser, C. I., & Rebelo, S. T. (2002). Production, Growth and Business Cycles: Technical Appendix. *Computational Economics*, *20*(1), 87–116. https://doi.org/10.1023/A:1020529028761

Lange, S. (2018). *Macroeconomics without Growth*. Metropolis-Verlag.

Lanz, B., Dietz, S., & Swanson, T. (2017). Global population growth, technology, and Malthusian constraints: A quantitative growth theoretic perspective. *International Economic Review*, *58*(3), 973–1006. https://doi.org/10.1111/iere.12242

Meadows, D. H., Meadows, D. L., Randers, J., & Behrens, W. (1972). *The Limits to Growth*. Universe Books.

OurWorldinData. (2023). *Multi-Year American Time Use Survey (2009-2019) – processed by Our World in Data. "With children" [dataset]. Multi-Year American Time Use Survey (2009-2019) [original data]*. Retrieved December 5, 2023, from https://ourworldindata.org/time-with-others-lifetime

Peretto, P. F., & Valente, S. (2015). Growth on a finite planet: Resources, technology and population in the long run. *Journal of Economic Growth*, *20*(3), 305–331. https://doi.org/10.1007/s10887-015-9118-z

Pullinger, M. (2014). Working time reduction policy in a sustainable economy: Criteria and options for its design. *Ecological Economics*, *103*, 11–19. https://doi.org/10.1016/j.ecolecon.2014.04.009

Raftery, A. E., & Ševčíková, H. (2023). Probabilistic population forecasting: Short to very long-term. *International Journal of Forecasting*, *39*(1), 73–97. https://doi.org/10.1016/j.ijforecast.2021.09.001

Saint-Paul, G. (2021). Secular satiation. *Journal of Economic Growth*, *26*(3), 291–327. https://doi.org/10.1007/s10887-021-09192-z

Smil, V. (2017). *Energy Transitions: Global and National Perspectives* (2nd ed.). Praeger.

Spencer, D. A. (2023). Marx, Keynes and the future of working time. *Cambridge Journal of Economics*. https://doi.org/10.1093/cje/bead046

Strulik, H. (2024). Long-run economic growth despite population decline. *Journal of Economic Dynamics and Control*, *168*, 104943. https://doi.org/10.1016/j.jedc.2024.104943

Strulik, H., Prettner, K., & Prskawetz, A. (2013). The past and future of knowledge-based growth. *Journal of Economic Growth*, *18*(4), 411–437. https://doi.org/10.1007/s10887-013-9098-9

Strulik, H., & Weisdorf, J. (2008). Population, food, and knowledge: A simple unified growth theory. *Journal of Economic Growth*, *13*(3), 195–216. https://doi.org/10.1007/s10887-008-9033-7

Tideman, T. N. (1982). A tax on land value is neutral. *National Tax Journal*, *35*(1), 109–111. https://doi.org/10.1086/NTJ41862425

UNESCO. (2021). *UNESCO Science Report: The race against time for smarter development*. https://www.unesco.org/reports/science/2021/en/download-report

United Nations. (2022). *World Population Prospects 2022, Online Edition* (Department of Economic and Social Affairs, Population Division). Department of Economic and Social Affairs, Population Division. https://population.un.org/wpp/Download/Standard/CSV/

Van Der Werf, E. (2008). Production functions for climate policy modeling: An empirical analysis. *Energy Economics*, *30*(6), 2964–2979. https://doi.org/10.1016/j.eneco.2008.05.008

Wang, F., Liao, H., & Tol, R. S. (2025). Baumol's climate disease. *European Economic Review*, *180*, 105175. https://doi.org/10.1016/j.euroecorev.2025.105175

A Derivation of the Social Planner Solution

The current-value Hamiltonian is

$$\begin{aligned}\mathcal{H} = {} & P(t)^{\theta} U\big(c(t), 1 - L_Z - L_E - L_n, n(t)\big) \\ & - \lambda(t)\big(E(t) - \bar{E}\big) \\ & + \mu_Y(t)\big(Y(t) - c(t)P(t) - I_Z(t) - I_E(t)\big) \\ & + \mu_Z(t)\big(I_Z(t) - \delta K_Z(t)\big) + \mu_E(t)\big(I_E(t) - \delta K_E(t)\big) \\ & + \mu_P(t)\big((n(t) - d)P(t)\big).\end{aligned}$$

Consumption. Taking the derivative with respect to $c(t)$ yields

$$\frac{\partial \mathcal{H}}{\partial c(t)} = P(t)^{\theta} U_c - \mu_Y(t) P(t) \stackrel{!}{=} 0.$$

Rearranging gives

$$\mu_Y(t) = P(t)^{\theta - 1} U_c. \tag{61}$$

Growth rate of $\mu_Y(t)$ is then given by

$$\frac{\dot{\mu}_Y(t)}{\mu_Y(t)} = (\theta - 1)\frac{\dot{P}(t)}{P(t)} + \frac{\dot{U}_c}{U_c}. \tag{62}$$

Capital in the intermediate sector. Taking the derivative with respect to $K_Z(t)$ yields

$$\frac{\partial \mathcal{H}}{\partial K_Z(t)} = \mu_Y(t) F_{K_Z}(t) - \mu_Z(t)\delta \stackrel{!}{=} \rho \mu_Z(t) - \dot{\mu}_Z(t).$$

Rearranging gives

$$F_{K_Z}(t) - \delta - \rho = -\frac{\dot{\mu}_Z(t)}{\mu_Z(t)} + \frac{\mu_Y(t) - \mu_Z(t)}{\mu_Z(t)} F_{K_Z}(t).$$

Taking the derivative with respect to $I_Z(t)$ yields

$$\frac{\partial \mathcal{H}}{\partial I_Z(t)} = -\mu_Y(t) + \mu_Z(t) \stackrel{!}{=} 0 \quad \Rightarrow \quad \mu_Z(t) = \mu_Y(t).$$

Substituting this into the capital equation gives

$$F_{K_Z}(t) - \delta - \rho = -\frac{\dot{\mu}_Y(t)}{\mu_Y(t)}. \tag{63}$$

Inserting eq. (62) gives the Euler-equation from the main text (eq. (15)):

$$F_{K_Z}(t) - \delta - \rho = (1-\theta)\frac{\dot{P}(t)}{P(t)} - \frac{\dot{U}_c}{U_c}. \tag{64}$$

Capital in the energy sector. Taking the derivative with respect to $K_E(t)$ yields

$$\frac{\partial \mathcal{H}}{\partial K_E(t)} = \mu_Y(t)F_{K_E}(t) - \mu_E(t)\delta - \lambda(t)E_{K_E}(t) \stackrel{!}{=} \rho\mu_E(t) - \dot{\mu}_E(t).$$

Taking the derivative with respect to $I_E(t)$ yields

$$\frac{\partial \mathcal{H}}{\partial I_E(t)} = -\mu_Y(t) + \mu_E(t) \stackrel{!}{=} 0 \quad \Rightarrow \quad \mu_E(t) = \mu_Y(t).$$

Inserting this into the capital condition gives

$$F_{K_E}(t) - \delta - \rho - \frac{\lambda(t)}{\mu_Y(t)}E_{K_E}(t) = -\frac{\dot{\mu}_Y(t)}{\mu_Y(t)}. \tag{65}$$

Inserting eqs. (61) and (62) gives the Euler-equation from the main text (eq. (17)):

$$F_{K_E}(t) - \delta - \rho - \frac{\lambda(t)}{P(t)^{\theta-1}U_c}E_{K_E}(t) = (1-\theta)\frac{\dot{P}(t)}{P(t)} - \frac{\dot{U}_c}{U_c}. \tag{66}$$

Labour in the intermediate sector. Taking the derivative with respect to $L_Z(t)$ yields

$$\frac{\partial \mathcal{H}}{\partial L_Z(t)} = P(t)^{\theta}U_{L_Z} + \mu_Y(t)F_{L_Z} = 0.$$

Substituting $\mu_Y(t) = P(t)^{\theta-1}U_c$ gives

$$F_{L_Z} = -\frac{U_{L_Z}}{U_c}P(t). \tag{67}$$

Labour in the energy sector. Taking the derivative with respect to $L_E(t)$ yields

$$\frac{\partial \mathcal{H}}{\partial L_E(t)} = P(t)^{\theta} U_{L_E} + \mu_Y(t) F_{L_E} - \lambda(t) E_{L_E} = 0.$$

Substituting $\mu_Y(t) = P(t)^{\theta-1} U_c$ and rearranging gives

$$F_{L_E} = -\frac{U_{L_E}}{U_c} P(t) + \lambda(t) \frac{E_{L_E}}{P(t)^{\theta-1} U_c} \tag{68}$$

Time rearing children. Using $n(t) = \kappa(t) L_n(t)^{\psi}$, taking the derivative with respect to $L_n(t)$ yields

$$\frac{\partial \mathcal{H}}{\partial L_n(t)} = P(t)^{\theta} U_{L_n} + \mu_P(t)\, P(t)\, \frac{\partial n(t)}{\partial L_n(t)} \stackrel{!}{=} 0,$$

where $\frac{\partial n(t)}{\partial L_n(t)} = \kappa(t) \psi L_n(t)^{\psi-1}$. Rearranging gives

$$\mu_P(t) = -P(t)^{\theta-1} \frac{U_{L_n}}{\kappa(t)} \psi L_n(t)^{\psi-1}. \tag{69}$$

Growth rate of $\mu_P(t)$ is then given by

$$-\frac{\dot{\mu}_P(t)}{\mu_P(t)} = (1-\theta)\frac{\dot{P}}{P} - \frac{\dot{U}_{L_n}}{U_{L_n}} - (1-\psi)\frac{\dot{L}_n}{L_n} + \frac{\dot{\kappa}}{\kappa} \tag{70}$$

Population. Taking the derivative with respect to $P(t)$ yields

$$\frac{\partial \mathcal{H}}{\partial P(t)} = \theta P^{\theta-1} U(\cdot) + \mu_Y(t)(F_P - c) - \lambda(t) E_P + \mu_P(t)(n-d) \stackrel{!}{=} \rho \mu_P(t) - \dot{\mu}_P(t).$$

Inserting eqs. (69) and (70) and rearranging leaves us with (eq. (19)) from the main text

$$\theta\frac{\dot{P}}{P} + \frac{\dot{U}_{L_n}}{U_{L_n}} - (\psi-1)\frac{\dot{L}_n}{L_n} - \frac{\dot{\kappa}}{\kappa} = \rho + \kappa\psi L_n^{\psi-1} \frac{U_c}{U_{L_n}} \left(\theta \frac{U(\cdot)}{U_c} + F_P - c - \frac{\lambda E_P}{P^{\theta-1} U_c} \right). \tag{71}$$

The transversality conditions are

$$\lim_{t\to\infty} e^{-\rho t} \mu_Y K_Z = 0, \qquad \lim_{t\to\infty} e^{-\rho t} \mu_Y K_E = 0, \qquad \lim_{t\to\infty} e^{-\rho t} \mu_P P = 0. \tag{72}$$

The Kuhn-Tucker Condition is given by

$$\lambda(t) \geq 0, \quad E(t) \leq \bar{E}, \quad \lambda(t)(E(t) - \bar{E}) = 0. \tag{73}$$

Equation (71) states the optimality condition in growth rates. For the anticipation argument in Section 6 it is useful to write the same condition in levels. The co-state equation for population is linear in $\mu_P(t)$ and can therefore be solved forward. Collecting the terms in $\mu_P(t)$ in the condition above gives

$$\dot{\mu}_P(t) - \left[\rho - (n(t) - d(t))\right] \mu_P(t) = -\Psi(t), \tag{74}$$

where, using the consumption first-order condition $\mu_Y = P^{\theta-1}U_c$,

$$\Psi(t) \equiv \mu_Y \left[\theta \frac{U}{U_c} + F_P - c - \lambda \frac{E_P}{P^{\theta-1}U_c}\right] \tag{75}$$

collects the instantaneous contributions of one additional person. The bracket in eq. (75) contains exactly the four components of the return to fertility listed after eq. (19).

Multiplying eq. (74) by the integrating factor $e^{-\int_0^t [\rho-(n-d)]\,ds}$ and integrating from t to T gives

$$\mu_P(t) = \int_t^T \Psi(\tau)\, e^{-\int_t^\tau \left[\rho-(n-d)\right] ds} d\tau + \mu_P(T) e^{-\int_t^T \left[\rho-(n-d)\right] ds}. \tag{76}$$

The terminal term is the transversality condition of eq. (72) in a different normalisation and vanishes as $T \to \infty$. Inserting eq. (69) on the left-hand side yields

$$-\frac{P(t)^{\theta-1}U_{L_n}}{\kappa\psi L_n(t)^{\psi-1}} = \int_t^\infty \mu_Y(\tau) \left[\theta \frac{U}{U_c} + F_P - c - \lambda \frac{E_P}{P^{\theta-1}U_c}\right] e^{-\int_t^\tau \left[\rho-(n-d)\right] ds} d\tau. \tag{77}$$

The marginal utility cost of time spent rearing children today equals the discounted stream of the net contributions of the resulting additional person. This includes the scarcity rent term, which enters the integrand at every future date at which the energy constraint binds. The shadow value of an additional person is therefore lower than in the unconstrained economy already today, and the shortfall grows as t approaches the binding date because the constrained phase is discounted less heavily.

B Proofs

B.1 Proof of Lemma 1

Proof. On a settled path, G converges to $\lim_{t\to\infty} G = g_{A_E} + \lim_{t\to\infty} g_P$. Three objects first. Since $aZ^\sigma > 0$ and raising to the negative power $1/\sigma$ reverses the inequality, output is bounded,

$$Y = \left(aZ^\sigma + b\bar{E}^\sigma\right)^{\frac{1}{\sigma}} < \left(b\,\bar{E}^\sigma\right)^{\frac{1}{\sigma}} = b^{\frac{1}{\sigma}}\bar{E} \equiv \bar{Y}, \tag{78}$$

and by (28) the energy share reaches one exactly at the bound. Substituting the factor payments $wL_Z = \alpha s_Z Y$ and $rK_Z = (1-\alpha)s_Z Y$ into the definition of Z gives the intermediate share in closed form,

$$s_Z = a\,(a\Theta)^{\frac{\sigma}{1-\sigma}}, \qquad \Theta \equiv (A_Z P)^\alpha\,\alpha^\alpha(1-\alpha)^{1-\alpha}\,w^{-\alpha}\,r^{-(1-\alpha)}, \tag{79}$$

strictly decreasing in Θ; with converging prices, $s_Z \to 0$ exactly when $A_Z P \to \infty$. Finally, since investment never exceeds output, $K_E(t) \le \bar{K} \equiv \max\{K_E(0), \bar{Y}/\delta\}$, and $\bar{E} = (A_E L_E P)^\nu K_E^{1-\nu}$ with $L_E \le 1$ requires

$$A_E(t)\,P(t) \;\ge\; \left(\bar{E}/\bar{K}^{1-\nu}\right)^{1/\nu} \;>\; 0 \tag{80}$$

while the cap binds.

If $\lim_{t\to\infty} G > 0$: $g_{A_Z} \ge g_{A_E}$ gives $g_{A_Z} + \lim_{t\to\infty} g_P > 0$, so $A_Z P \to \infty$, $\Theta \to \infty$, $s_Z \to 0$, and $Y \to \bar{Y}$. The intermediate payments $\alpha s_Z Y$ and $(1-\alpha)s_Z Y$ then vanish, and the positive price limits force $L_Z \to 0$ and $K_Z \to 0$. Settled growth rates with positive finite price limits give $g_w = g_r = 0$, so $D \to 0$, and by (39) and (40) both energy inputs decline at the rate $\nu \lim_{t\to\infty} G > 0$ and vanish. In (34) the factor terms vanish while $Y \to \bar{Y}$, so $s_R \to 1$ and $q = s_R Y/\bar{E} \to b^{1/\sigma}$; work time vanishes, so $l \to 1 - \lim_{t\to\infty} L_n$. Investment $I_i = K_i(g_{K_i} + \delta)$ vanishes with the capital stocks, and the aggregate resource constraint gives $C \to \bar{Y}$. If $\lim_{t\to\infty} G < 0$: $A_E P \to 0$, so (80) fails in finite time and no capped BGP exists. □

B.2 Proof of Proposition 1

Proof. The fertility choice of the social planner is governed by the optimality condition for population (19), shown here again with the rent q from (29) replacing the multiplier,

$$\theta\frac{\dot{P}}{P}+\frac{\dot{U}_{L_n}}{U_{L_n}}+(1-\psi)\frac{\dot{L}_n}{L_n}-\frac{\dot{\kappa}}{\kappa}=\rho+\kappa\psi L_n^{\psi-1}\frac{U_c}{U_{L_n}}\left(\theta\frac{U}{U_c}+F_P-c-qE_P\right). \tag{81}$$

Inserting the marginal utilities implied by (7), using $n=\kappa L_n^{\psi}$ and the time constraint (8), together with the marginal products of population at the binding cap, $F_P=(\alpha s_Z+\nu s_E)\,Y/P$ and $E_P=\nu\bar{E}/P$, the rent share $s_R=q\bar{E}/Y$ from (34), and the factor payments $wL_Z=\alpha s_Z Y$ and $wL_E=\nu\,(s_E-s_R)\,Y$ from (29) and (36) gives

$$\begin{aligned}&\theta g_P+(1-\eta)\,(g_x+\gamma g_l+\epsilon g_n)+\frac{\gamma L_n\,g_l-\epsilon\psi\,l\,g_{L_n}}{\epsilon\psi\,l-\gamma L_n}+(1-\psi)g_{L_n}-g_\kappa\\&=\rho+\frac{\psi\,n\,l}{x\,(\epsilon\psi\,l-\gamma L_n)}\left(\theta\left[\frac{x}{1-\eta}+B\,x^{\eta}\right]+\frac{w(L_Z+L_E)}{P}-c\right),\end{aligned}$$

where $x\equiv c-\bar{c}$ and $B\equiv\bar{u}\,l^{\gamma(\eta-1)}n^{\epsilon(\eta-1)}>0$.

By Lemma 1 a capped BGP requires $\lim_{t\to\infty}G\geq 0$, and $\lim_{t\to\infty}G=0$ is a knife edge we do not characterize, so work vanishes and the economy settles: $g_l=g_n=g_{L_n}=g_\kappa=0$, leisure absorbs the freed time, $l=1-L_n$, and the labor income term drops out, since inserting the wage $w=\gamma(c-\bar{c})P/l$ from (29) makes its contribution proportional to $L_Z+L_E\to 0$. The condition reduces to

$$\theta g_P+(1-\eta)g_x=\rho+\frac{\psi\,n\,l}{x\,(\epsilon\psi\,l-\gamma L_n)}\left(\theta\left[\frac{x}{1-\eta}+B\,x^{\eta}\right]-c\right),$$

where the time allocation, n, and $\kappa=\bar{\kappa}$ stand at their long-run values while consumption and population may still move. Since $C\leq Y<\bar{Y}$ by (78) and $c\geq\bar{c}$, population is bounded, $P\leq\bar{Y}/\bar{c}$: no capped BGP has $n>\bar{d}$, so population is either stationary, $n=\bar{d}$, or declining, $n<\bar{d}$, the two parts of the proposition.

1. Stationary population: here $g_P=0$, and $\lim_{t\to\infty}G=g_{A_E}>0$, so case (i) of Lemma 1 delivers the full leisure economy; $C\to\bar{Y}$ with constant population makes consumption converge, $g_x=0$ and $P^*=\bar{Y}/c^*$. Replacement pins $n=\bar{d}$, $L_n=L_n^*$, and $l^*=1-L_n^*$ from (52). Both sides of the reduced condition are then constants; multiplying by $x\,(\epsilon\psi\,l^*-\gamma L_n^*)\,/(\psi\,\bar{d}\,l^*)$ and using $(\epsilon\psi\,l^*-\gamma L_n^*)/l^*=$

$\epsilon\psi - \gamma L_n^*/(1 - L_n^*)$ rearranges it to (53). A stationary level is therefore a positive root of

$$\Phi(x) \equiv (x + \bar{c}) - \theta\left(\frac{x}{1-\eta} + Bx^{\eta}\right) - Rx,$$

with B evaluated at $(l^*, \bar{d})$, and $\Phi(0) = \bar{c} > 0$ because both terms of $\theta U/U_c = \theta(x/(1-\eta) + Bx^{\eta})$ vanish at $x = 0$.

(a) $\theta = 0$: Φ is affine with slope $1 - R$: a positive root exists if and only if $R > 1$, at $x^* = \bar{c}/(R-1)$, that is $c^* = \bar{c}R/(R-1)$.

(b) $\theta > 0$: $\Phi'' = -\theta B\eta(\eta - 1)x^{\eta-2} < 0$, and since $\eta > 1$ the existence-value term $-\theta Bx^{\eta}$ outgrows every linear term, so $\Phi \to -\infty$: a strictly concave function that starts at $\bar{c} > 0$ and eventually falls below zero crosses zero exactly once, for any R. For the second claim, consider a capped BGP with declining population and $\theta > 0$. Marginal utility diverges in each argument of (7), so the path is interior; the wage limit makes $(c - \bar{c})P = wl/\gamma$ converge to a positive constant, so the surplus grows at $g_x = -\hat{g}_P > 0$, $x \to \infty$, and $c/x \to 1$. In the reduced condition the left side is a constant, and so is the limit of every right-side term except the existence value, whose contribution $\psi\, n\, l\, \theta B\, x^{\eta-1}/\left(\epsilon\psi\, l - \gamma L_n\right)$ diverges since $\eta > 1$: no such path satisfies the condition.

2. Declining population for $\theta = 0$: let $R < 1$; no stationary population exists by part 1a, and growing population is infeasible, so any capped BGP has $n < \bar{d}$. As in part 1b, the wage limit gives $g_x = g_c = -\hat{g}_P > 0$ and $c/x \to 1$. Taking the limit of the reduced condition with $\theta = 0$, $n = \bar{\kappa}\hat{L}_n^{\psi}$, and $\hat{l} = 1 - \hat{L}_n$ gives

$$(1 - \eta)\, g_c = \rho - \psi\, \bar{\kappa}\hat{L}_n^{\psi}\left[\epsilon\psi - \gamma\, \frac{\hat{L}_n}{1 - \hat{L}_n}\right]^{-1};$$

substituting $g_c = \bar{d} - \bar{\kappa}\hat{L}_n^{\psi}$ and rearranging gives (54). On the range where both sides are positive, the left side falls strictly and the right side rises strictly; at $L_n \to 0$ they equal $\epsilon\psi > 0$ and zero, and at the range's upper end the left side reaches zero or the right side diverges, so they cross exactly once. At L_n^* the right side's denominator equals ρ and the ratio of the sides equals R; $R < 1$ places the root below L_n^*, so $\hat{g}_P < 0$; roots above L_n^* would imply $n > \bar{d}$ and are infeasible.

Parts 2a and 2b: if $g_{A_E} + \hat{g}_P > 0$, case (i) of Lemma 1 delivers the full leisure economy, with per-capita consumption growing at $-\hat{g}_P$ as shown. If $g_{A_E} + \hat{g}_P < 0$, case (ii) applies: no capped BGP exists, and the cap ceases to bind in finite time.

□

C Calibration

C.1 Derivation of $\bar{u}$

Adhami et al. (2023) calculate $v(c)$ as the value of a year of life, measured in dollars, as a ratio to consumption per person. Their benchmark result states that a year of life in 2006 in the United States is valued at approximately 5 years worth of consumption per person (Adhami et al., 2023, p.8), so that

$$v(c) \equiv \frac{U(c)}{U_c c} \stackrel{!}{=} v(c_{us,2006}) = 4.87. \tag{82}$$

For our model setup we follow their approach analogously with our utility function given by Equation (7) and find that

$$v(c,l,n) \equiv \frac{U(c,l,n)}{U_c c} = \frac{(c-\bar{c})}{(1-\eta)c} + \frac{\bar{u}}{(c-\bar{c})^{-\eta} l^{\gamma(1-\eta)} n^{\epsilon(1-\eta)} c}. \tag{83}$$

By equating Equation (82) with Equation (83) we can rearrange to obtain

$$\bar{u} = \left(4.87 - \frac{(c-\bar{c})}{(1-\eta)c}\right)(c-\bar{c})^{-\eta} l^{\gamma(1-\eta)} n^{\epsilon(1-\eta)} c. \tag{84}$$

Using our benchmark calibration and 2006 US values for fertility, $n_{2006,US} = 0.0142$ (Hamilton et al., 2007), leisure, $l_{2006,US} = 0.396$[6] (Bureau of Labor Statistics, 2007), and consumption, $c_{2006,US} = 36.76$ thousand$ (FRED, 2024), we obtain

$$\bar{u} = \left(4.87 - \frac{(36.76 - 0.365)}{(1-1.35)36.76}\right)(36.76 - 0.365)^{-1.35} 0.396^{0.818\cdot(1-1.35)} 0.0142^{1\cdot(1-1.35)} 36.76 = 12.8,$$

[6] Leisure is defined as: Leisure and Sports + Educational Activities + Organizational, civic, and religious activities + Other activities, not elsewhere classified, which equals 6.09 hours per day for the average American in 2006. We divide this number by the hours per day minus sleeping time of 8.63, so that we receive $l_{2006,US} = 6.09/(24 - 8.63) = 0.396$.

which is higher than the value of Adhami et al. (2023). For $\theta = 0$, the parameter $\bar{u}$ is an additive constant in the planner's objective and does not affect any allocation; it matters only for the total utilitarian planner.

C.2 Fertility and Mortality

Fertility Fertility costs are estimated by running a non-linear regression in R for the cost parameter $\kappa(t)$ given by

$$\kappa(t) = \frac{n(t)}{\bar{L}_n^{\psi}} = \kappa_0 e^{-g_\kappa t} + \bar{\kappa}. \tag{85}$$

Since ψ is jointly calibrated in the grid search (see Section C.3), the estimation of $(\kappa_0, \bar{\kappa})$ is repeated for each candidate value of $\psi \in [0.10, 1.00]$, with g_κ estimated in a first stage and held fixed across ψ (rescaling by $\bar{L}_n^{-\psi}$ multiplies $\kappa(t)$ by a constant and leaves g_κ unchanged). Table 6 reports the results for $\psi = 0.30$ (the best-fit value) and the resulting fitted path is plotted in Figure 7.

Table 6: Estimation results for the cost parameter $\frac{n(t)}{\bar{L}_n^{\psi}}$ with $\psi = 0.30$.

Parameter	Estimate	Std. Error	t value	p-value
κ_0	0.0553295	0.0004732	116.93	$< 2 \times 10^{-16}$
g_κ	0.0183405	0.0005445	33.68	$< 2 \times 10^{-16}$
$\bar{\kappa}$	0.0152850	0.0002094	73.00	$< 2 \times 10^{-16}$

Mortality The baseline mortality path $d_{\text{base}}(t)$ is estimated by running a non-linear regression in R for the specification in Equation (55). The results are displayed in Table 7 and plotted in Figure 8. The full mortality function used in the model is then given by

$$d(t) = d_0 e^{-g_d t} + \frac{d_{\text{UN}}}{1 + e^{-m_1 (t - t_1)}} - \frac{d_{\text{UN}} - \bar{d}}{1 + e^{-m_2 (t - t_2)}}. \tag{86}$$

The correction term activates smoothly around t_2 with steepness m_2, shifting the mortality path from the UN-fitted baseline toward $\bar{d}$ in the long run. For $t \ll t_2$, the correction is negligible and $d(t) \approx d_{\text{base}}(t)$, preserving the empirical fit over the historical and near-future period. For $t \gg t_2$, the correction converges to $d_{\text{UN}} - \bar{d}$, so

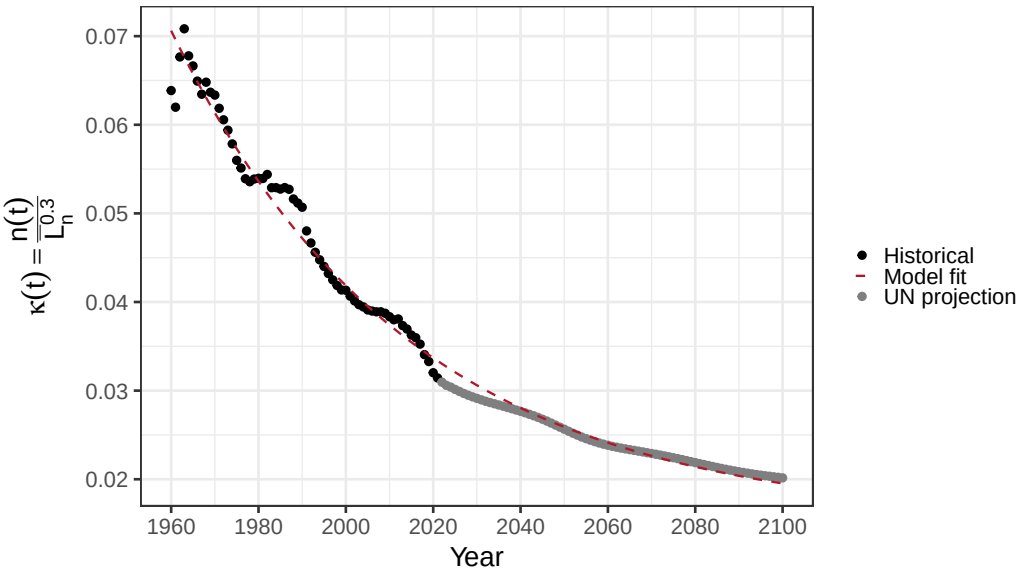


Figure 7: Estimation results for the cost parameter $\kappa(t)$ versus data on fertility.

that $d(t) \to d_0 e^{-g_d t} + \bar{d}$. We set $t_2 = 200$ (year 2160) and $m_2 = 0.05$, which ensures a gradual transition that leaves the pre-2100 fit virtually undisturbed. Because the crude death rate embeds the age composition of the UN baseline, and we hold the same path fixed across counterfactuals whose fertility differs, the resulting population paths are reduced-form scenarios rather than age-consistent demographic projections.

Figure 8 displays historical mortality data, UN projections up until 2100 and our calibrated model mortality rate with different future projections (eq. (86)). The non-monotonic shape of the mortality path reflects two opposing forces on the crude death rate. The advancement effect captures medical and economic progress: age-specific mortality falls over time, which pushes the death rate down and dominates the historical period. The composition effect works in the opposite direction: as fertility declines and longevity rises, the population shifts toward older age groups with higher mortality, so the crude death rate rises even though mortality for every age group declines. The composition effect dominates from around 2020 onward, which is why the mortality rate falls until 2020 and then rises, before settling at the long-run scenario rate.

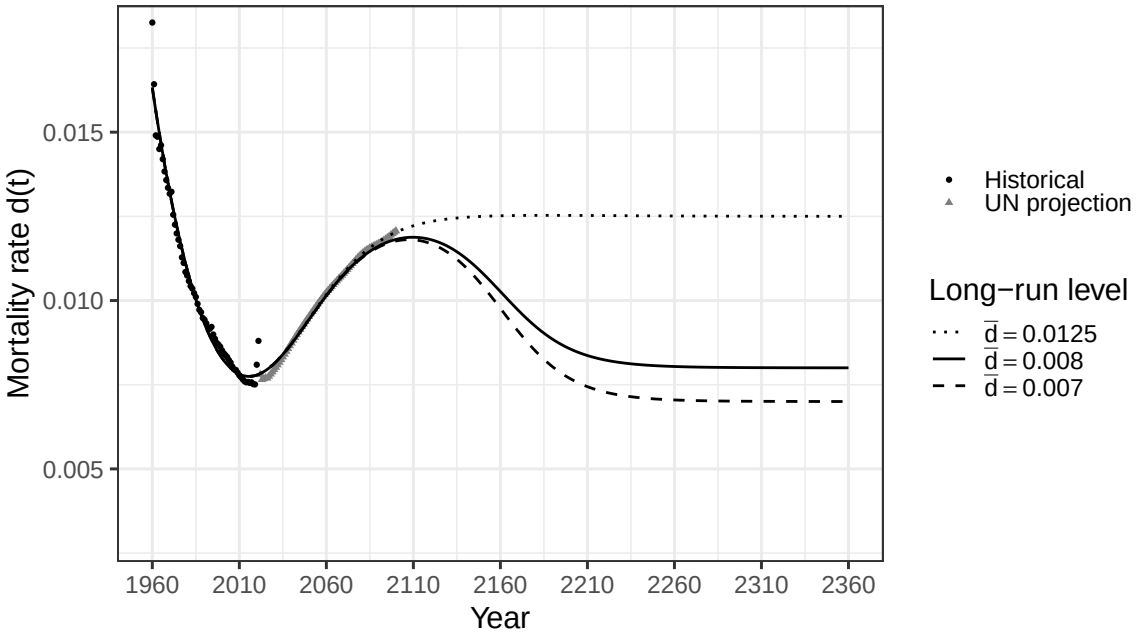


Figure 8: Historical and Projected Mortality Rate

Table 7: Estimation results for the baseline mortality path $d_{\text{base}}(t)$.

Parameter	Estimate	Std. Error	t value	p-value
d_0	0.01581403	0.00009679	163.39	$< 2 \times 10^{-16}$
g_d	0.02368185	0.00080706	29.34	$< 2 \times 10^{-16}$
d_{UN}	0.01245200	0.00022865	54.46	$< 2 \times 10^{-16}$
m_1	0.03996038	0.00186621	21.41	$< 2 \times 10^{-16}$
t_1	78.98450148	0.98321224	80.33	$< 2 \times 10^{-16}$

C.3 Grid Search

The internal calibration searches over $(\psi, g_{A_Z}, g_{A_E}, s)$ on the grid reported in Table 8, with a locally refined step for s above 0.80, $\epsilon = 1$ as a normalization, and γ chosen to match the 2006 leisure share. For each value of ψ, the fertility cost parameters $(\kappa_0, \bar{\kappa})$ are re-estimated as described in the fertility calibration above.

Table 8: Grid ranges for the internal calibration

Parameter	Description	Range
ψ	Decreasing returns in fertility	$0.10, \ldots, 1.00$ (step 0.05)
g_{A_Z}	Productivity growth (final good)	$0.010, \ldots, 0.030$ (step 0.001)
g_{A_E}	Productivity growth (energy)	$0.000, \ldots, 0.02$ (step 0.001)
s	Substitution (energy–non-energy)	$0.10, \ldots, 0.90$ (step 0.05)

Search procedure The loss surface is searched by a sequential coordinate procedure: first ψ, then g_{A_Z}, then $g_{A_E} \times s$, each stage holding the other parameters at their current values. Because such a procedure can depend on its starting point, it is run from twelve starting points that span the admissible ranges by construction, $g_{A_Z} \in \{0.015, 0.025\}$, $g_{A_E} \in \{0, 0.01\}$, and $s \in \{0.3, 0.6, 0.9\}$, and each run is iterated twice. Ten of the twelve runs terminate at the identical parameter vector and the remaining two at a neighboring grid point with an indistinguishable loss, so the reported optimum does not depend on where the search starts. The leisure weight γ is then chosen so that the model's 2006 leisure share equals the time-use value of 0.396 (bisection), followed by a local refinement of (ψ, g_{A_Z}, s).

Identification of the fertility preference The data identify the preference for children only through the composite $\epsilon\psi$, which governs the share of time devoted to child-rearing in the planner's time-allocation condition, in the same way that γ governs the leisure share. The fit is flat along combinations of ϵ and ψ that hold this composite near 0.30, so ϵ is not separately identified, and we normalize $\epsilon = 1$. The calibrated model implies a child-rearing time share of 0.130 in 2006, close to the value of 0.125 in the US time use data — a moment the calibration does not target.

Solver protocol Each grid point is a non-convex dynamic optimization problem, and inferior local optima can produce time paths that spuriously resemble the data.

Two safeguards address this: neighboring grid points are solved in sequence with warm starts, which keeps solutions on a continuous branch, and the top twenty candidates are re-solved from an alternative starting point and ranked at their highest-welfare solution before the fit is compared. Calibration solves use a 300-year horizon; extending it to 500 years changes the loss by less than 10^{-9}, and varying the post-2100 mortality scenario changes it by less than 10^{-3} relative. The full procedure requires roughly 10,600 model solutions.

D Sensitivity Analysis

D.1 Different Limits on Energy

We vary the upper bound on energy supply $\bar{E}$ across five values: 5,000, 7,500, 10,000, 15,000, and 20,000 EJ. Figure 9 shows that the qualitative mechanisms described in Section 6 are robust: variations in $\bar{E}$ primarily shift the timing at which the constraint becomes binding and, consequently, the speed of the transition toward the leisure economy.

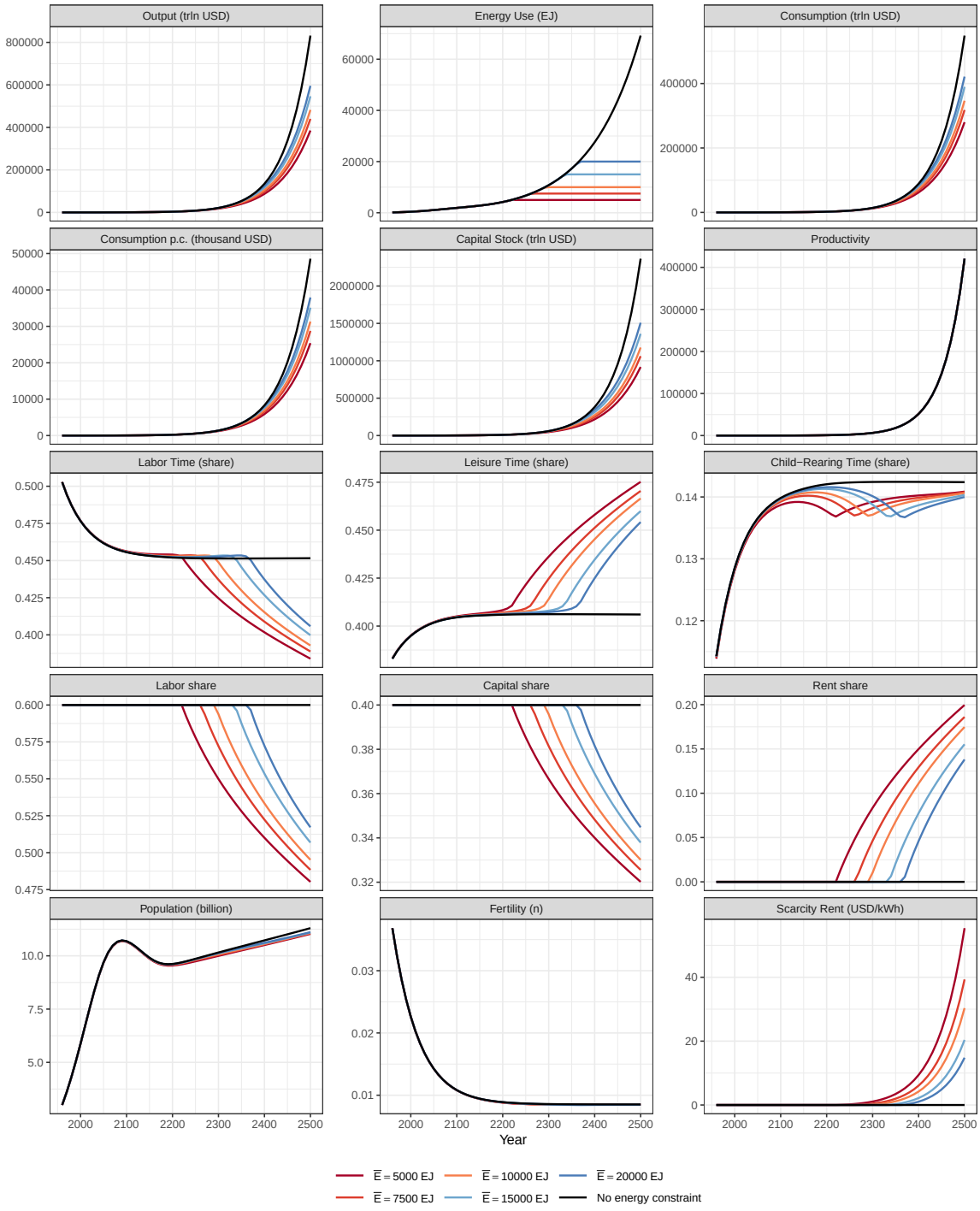


Figure 9: Sensitivity to the energy limit $\bar{E}$. Average utilitarian ($\theta = 0$).

D.2 Substitution Elasticity between Intermediates and Energy

We vary the elasticity of substitution s between intermediates and energy across three values: $s = 0.20$, $s = 0.50$, and $s = 0.90$ (the calibrated baseline). Lower values of s correspond to stronger complementarity between intermediates and energy in production: when s is small, energy cannot easily be substituted by other inputs and a fall in available energy translates more directly into a fall in output. As s approaches unity, the production technology approaches Cobb–Douglas, allowing intermediates to compensate more flexibly for scarce energy.

Figure 10 shows the unconstrained case. Stronger complementarity ties output more closely to energy, so the low-s economies produce substantially less output and consume more energy per unit of output. Per-capita consumption grows more slowly and the time allocation adjusts slightly.

Figure 11 repeats the exercise with a binding energy constraint at $\bar{E} = 10{,}000$ EJ. Stronger complementarity increases energy consumption, so the constraint binds earlier. However, the $s = 0.20$ and $s = 0.50$ paths cross around 2430, both in the time allocation and in the income shares.

The crossing arises because s affects the two components of the transition in opposite directions. The rent share equals the energy share minus the payments to labor and capital used to provide the fixed energy flow. The transition to the leisure economy proceeds as the energy share rises and the input payments fall. On the one hand, a lower s raises the energy share faster: after the cap binds it grows with elasticity $(1-s)/s$, which is four at $s = 0.20$, one at $s = 0.50$, and one ninth at the baseline. On the other hand, a lower s increases the input payments. With high substitutability, the output bound $\bar{Y} = b^{1/\sigma}\bar{E}$ lies far above current output, so output continues to grow at almost its previous rate after the cap binds. This output finances investment in energy capital, and the rising wage $w = \gamma(c - \bar{c})/l$ makes substituting capital for labor profitable. With low substitutability, the bound is close and output reaches it within about a century of the binding date. Investment in energy capital is small, wages remain low, and a large workforce continues to provide the fixed flow, with payments declining only at the rate of energy productivity growth.

The $s = 0.20$ economy therefore adjusts quickly at first and then slows down: its energy share is close to one by 2500, but its input payments remain substantial. The $s = 0.50$ economy continues to adjust on both components and overtakes it around 2430. Stronger complementarity thus advances the binding date but slows the subsequent

transition. Beyond the displayed horizon all three economies converge to the full leisure economy, since the effective energy workforce keeps growing in every run (Lemma 1).

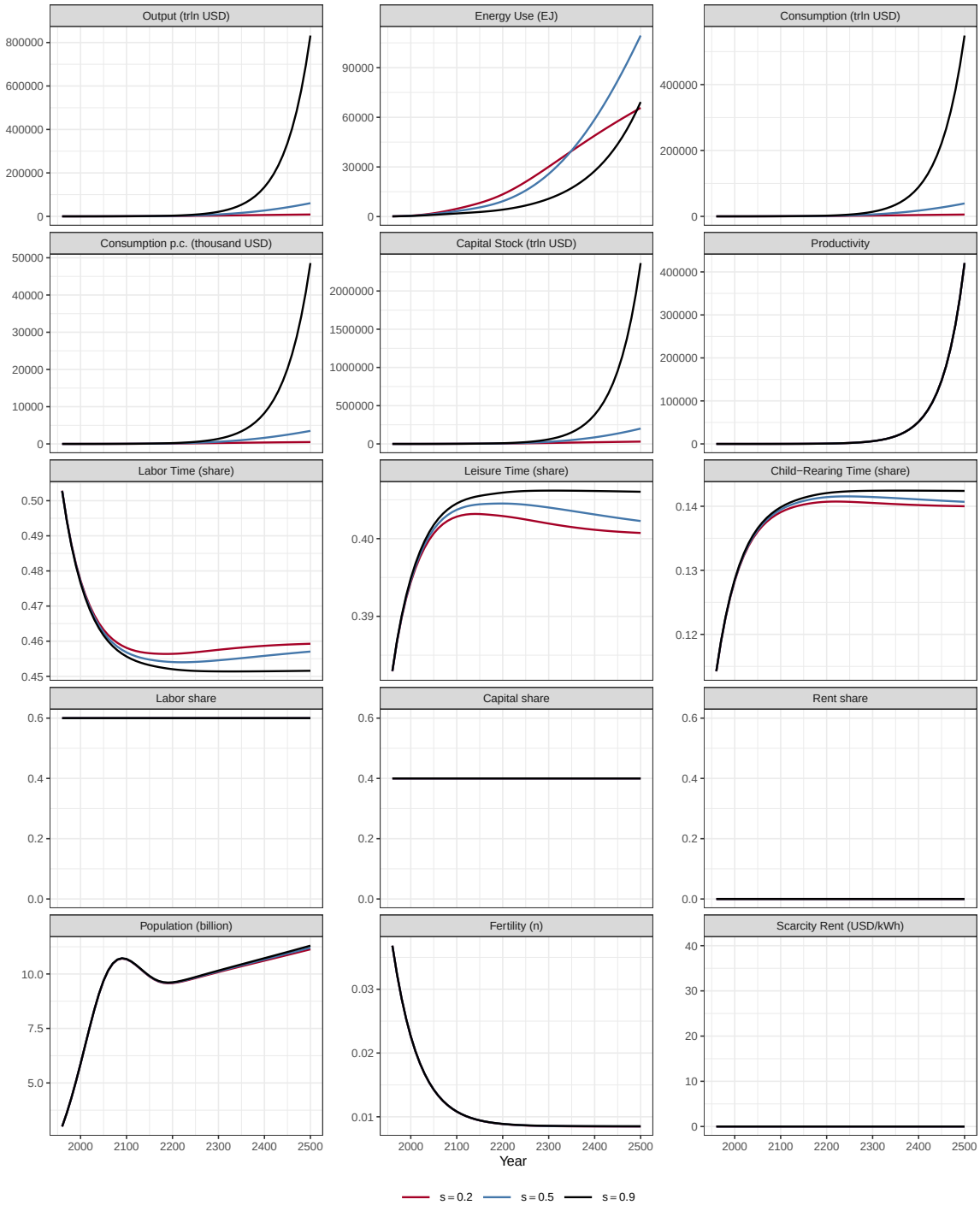


Figure 10: Sensitivity to the substitution elasticity s between intermediates and energy. Average utilitarian ($\theta = 0$). No energy constraint.

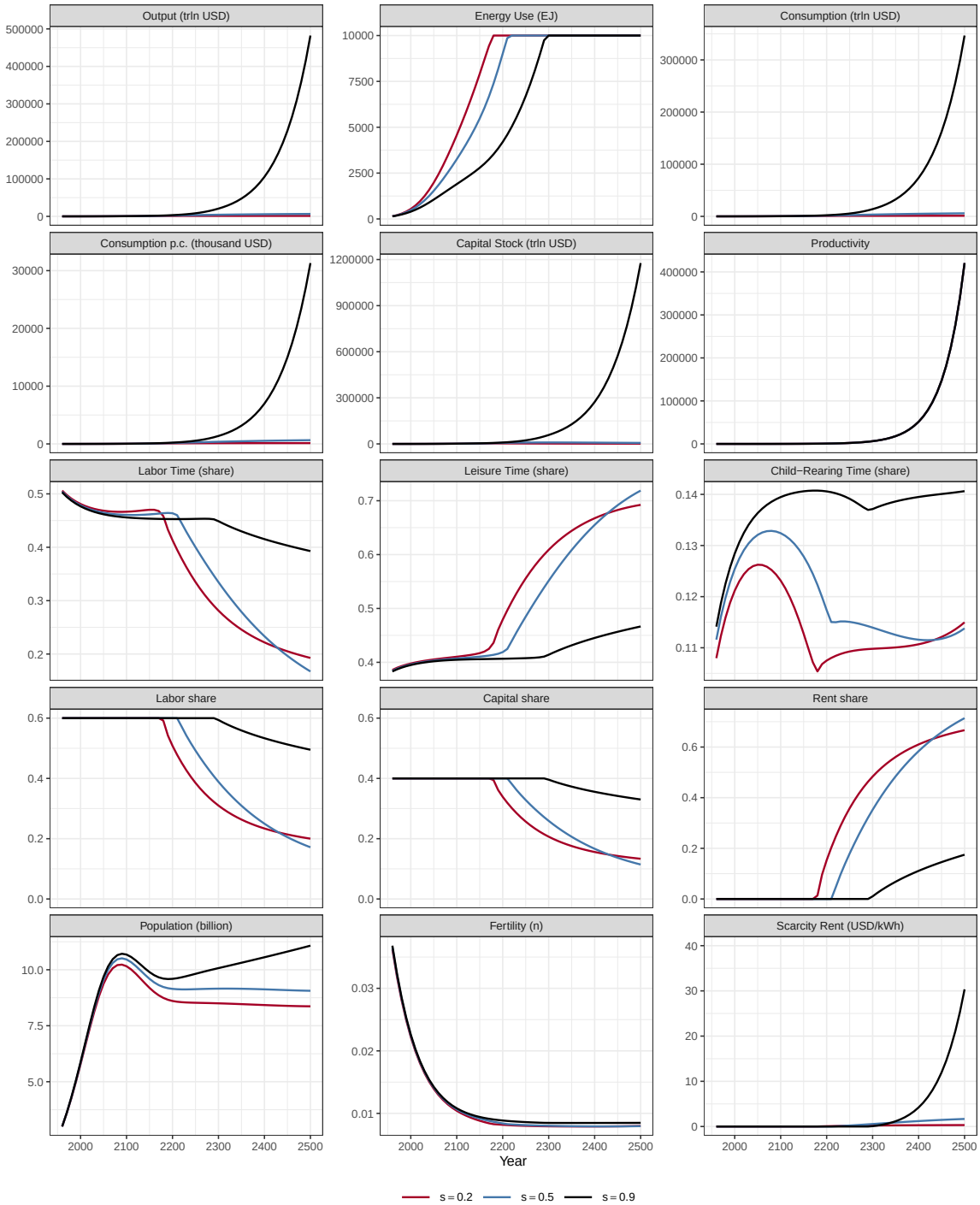


Figure 11: Sensitivity to the substitution elasticity s between intermediates and energy. Average utilitarian ($\theta = 0$). Energy constraint at $\bar{E} = 10{,}000$ EJ.

D.3 Different Mortality Scenarios

We vary the long-run death rate $\bar{d}$ across the three scenario values of Section 5: 0.007, under which population keeps rising, the baseline 0.008, at which it is approximately stationary, and $\bar{d} = d_{\text{UN}} = 0.0125$, under which mortality stays at its projected 2100 level and population declines. Since $\bar{d}$ only affects the mortality path after 2100 via the smooth double-logistic transition described in Section C.2, the calibration on 1960–2020 data is unaffected.

Figure 12 shows results without an energy constraint. Lower $\bar{d}$ implies lower long-run mortality and therefore higher population, which in turn raises aggregate output and energy demand. This is expected since these variables scale with population. Intensive variables like the labor time and leisure share or consumption per-capita are unaffected.

Figure 13 repeats this exercise with the energy constraint at $\bar{E} = 10{,}000$ EJ. On the transition, larger populations reach the cap earlier: the binding date moves from 2290 at $\bar{d} = 0.007$ to 2300 in the baseline and about 2450 at $\bar{d} = 0.0125$.

In the long run, the three scenarios select the three futures of Section 4, as announced in Section 5. At $\bar{d} = 0.007$ the replacement value in (53) exceeds one ($R = 1.12$). Although the displayed paths still show a rising population, the planner sustains a stationary population in the long run — future (i). The baseline $\bar{d} = 0.008$ gives $R = 0.81$ with a positive G, future (ii), as reported in Section 6.1. At $\bar{d} = 0.0125$ the settled population decline of 0.47 percent per year outruns energy-augmenting productivity growth, so $G < 0$ and by Proposition 1 no permanently capped path exists — future (iii), in which the cap eventually stops binding. However, the unbinding itself lies past the simulated horizon.

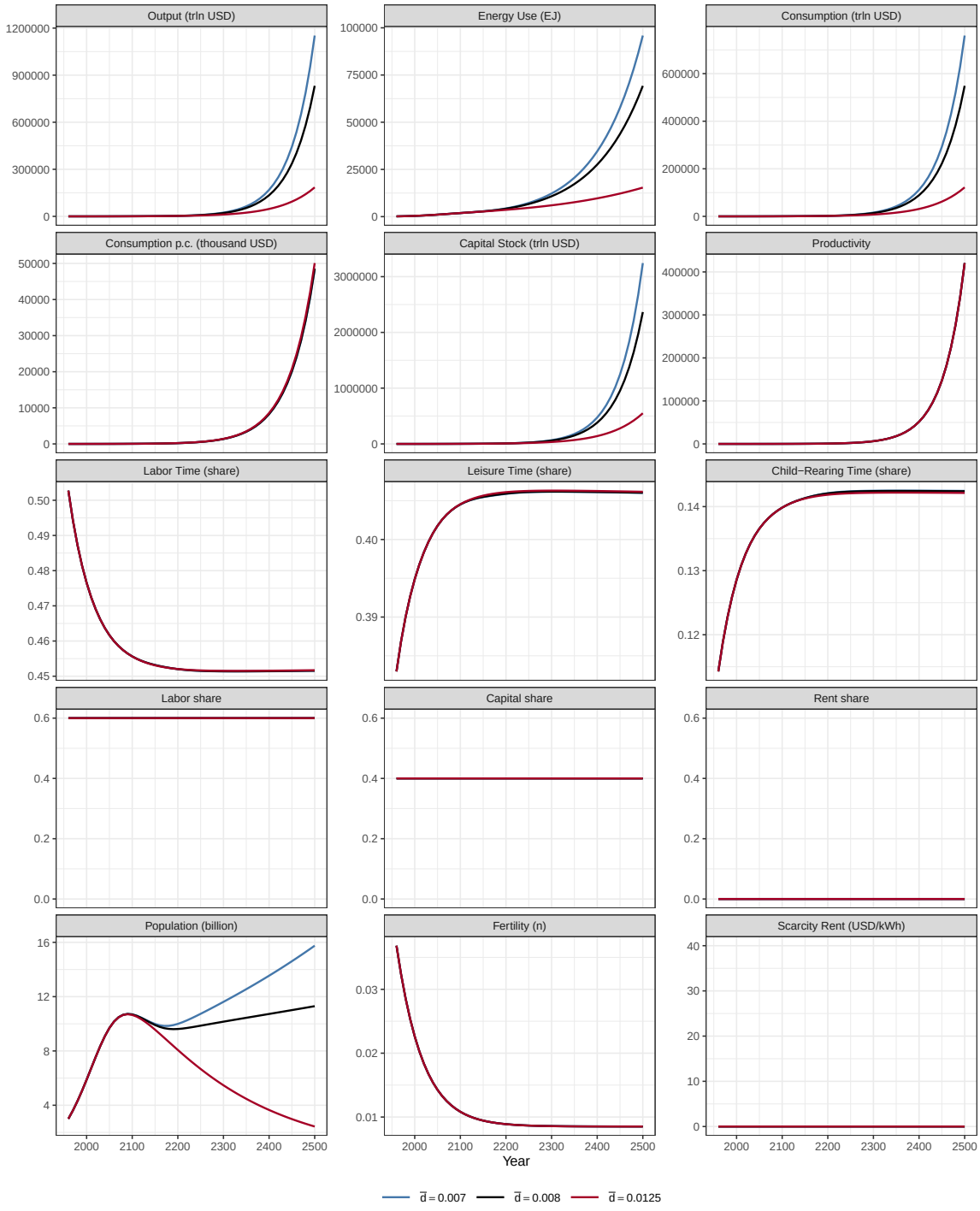


Figure 12: Sensitivity to the mortality floor $\bar{d}$. Average utilitarian ($\theta = 0$). No energy constraint.

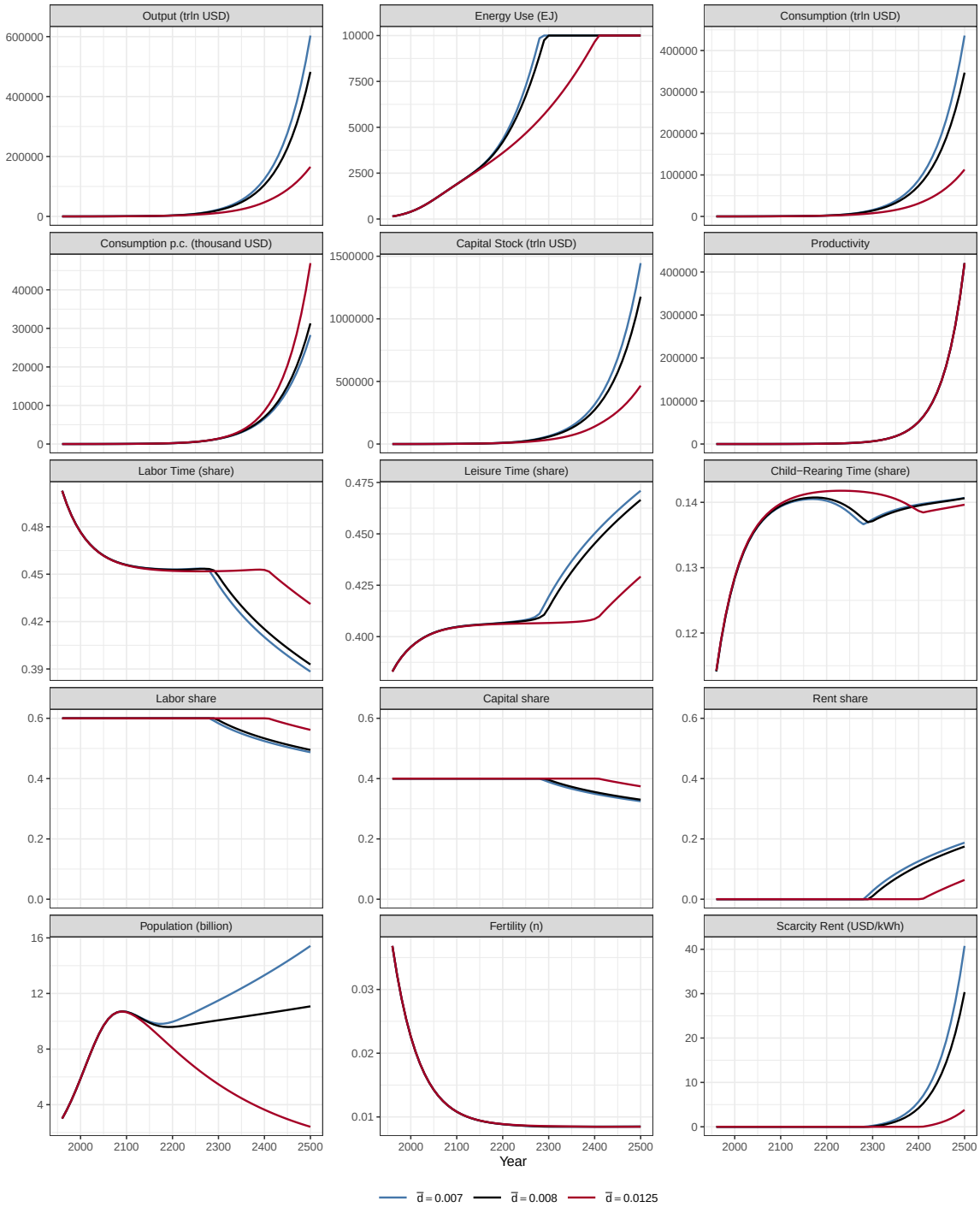


Figure 13: Sensitivity to the mortality floor $\bar{d}$. Average utilitarian ($\theta = 0$). Energy constraint at $\bar{E} = 10{,}000$ EJ.

E Endogenous Growth

This section presents the full model setup and first-order conditions for the economy with endogenous growth. Furthermore, we present the normalization of the scale parameters ζ_i. They are evaluated at the observed 2020 research inputs, and must deliver the observed 2020 productivity growth rates,

$$\zeta_i = \frac{g_{A_i}(2020)\, A_i(2020)^{\beta_i}}{\left(L_{R,i}^{\text{obs}} P(2020)\right)^{\omega_i}}, \tag{87}$$

where $A_i(2020)$ and $P(2020)$ are the baseline model's 2020 levels ($A_Z = 17.6$, $A_E = 191.1$, $P = 7.56$ billion) and $g_{A_i}(2020)$ its 2020 growth rates (2.1% for the intermediate sector, 0.1% for energy). We measure the observed research share $L_{R,i}$ from headcounts: there are about 8.9 million full-time-equivalent researchers worldwide and 15 million when accounting for technicians and support staff (UNESCO, 2021). Global employment is roughly 3.4 billion according to ILO, so that roughly 0.44% of the workforce are in research. Scaling this by the model's work-time share of roughly 45% gives roughly $L_{R,Z}^{\text{obs}} = 0.002$. We assume that energy accounts for about a tenth of global R&D, so $L_{R,E}^{\text{obs}} = 0.0002$. This then gives $\zeta_Z = 12.6$ for the intermediate sector, and for the energy sector $\zeta_E = 0.073$ at $\beta_E = 0.2$ and $\zeta_E = 67.9$ at $\beta_E = 1.5$.

E.1 Extended Model Setup

Productivity in the intermediate good sector evolves according to

$$\dot{A}_Z(t) = \zeta_Z \left(L_{R,Z}(t) P(t)\right)^{\omega_Z} A_Z(t)^{1-\beta_Z}, \tag{88}$$

while productivity in the energy sector evolves according to

$$\dot{A}_E(t) = \zeta_E \left(L_{R,E}(t) P(t)\right)^{\omega_E} A_E(t)^{1-\beta_E}. \tag{89}$$

Here, ζ_i is a scaling parameter, ω_i captures duplication among researchers (we set $\omega_Z = \omega_E = \omega$), and β_i captures the extent to which ideas become harder to find in sector $i \in \{Z, E\}$.

The time constraint now reads

$$1 = L_Z(t) + L_E(t) + L_n(t) + L_{R,Z}(t) + L_{R,E}(t) + l(t). \tag{90}$$

The rest of the model remains unchanged.

E.1.1 Hamiltonian

The current-value Hamiltonian is

$$\begin{aligned}\mathcal{H} = {} & P(t)^\theta U\big(c(t), 1 - L_Z - L_E - L_n - L_{R,Z} - L_{R,E}, n(t)\big) \\ & - \lambda(t)\big(E(t) - \bar{E}\big) \\ & + \mu_Y(t)\big(Y(t) - c(t)P(t) - I_Z(t) - I_E(t)\big) \\ & + \mu_Z(t)\big(I_Z(t) - \delta K_Z(t)\big) + \mu_E(t)\big(I_E(t) - \delta K_E(t)\big) \\ & + \mu_P(t)\big((n(t) - d)P(t)\big) \\ & + \mu_{A_Z}(t)\zeta_Z\big(L_{R,Z}(t)P(t)\big)^{\omega_Z} A_Z(t)^{1-\beta_Z} \\ & + \mu_{A_E}(t)\zeta_E\big(L_{R,E}(t)P(t)\big)^{\omega_E} A_E(t)^{1-\beta_E}.\end{aligned}$$

E.1.2 Optimality Conditions

Optimality Conditions for capital, labor and consumption are the same as in the model with exogenous growth. However, we receive new optimality conditions for research in both sectors as well as a different optimality condition for population.

Research labour in the intermediate sector. Taking the derivative with respect to $L_{R,Z}(t)$ yields

$$\begin{aligned}\frac{\partial \mathcal{H}}{\partial L_{R,Z}(t)} = {} & P(t)^\theta U_{L_{R,Z}}(t) \\ & + \mu_{A_Z}(t)\zeta_Z\omega_Z\big(L_{R,Z}(t)P(t)\big)^{\omega_Z - 1} P(t) A_Z(t)^{1-\beta_Z} = 0.\end{aligned}$$

Using $U_{L_{R,Z}}(t) = -U_l(t)$ gives

$$P(t)^\theta U_l(t) = \mu_{A_Z}(t)\zeta_Z\omega_Z P(t)^{\omega_Z} L_{R,Z}(t)^{\omega_Z - 1} A_Z(t)^{1-\beta_Z}, \tag{91}$$

which can be rearranged to receive

$$\mu_{A_Z}(t) = \frac{U_l(t)}{\zeta_Z \omega_Z} P(t)^{\theta-\omega_Z} L_{R,Z}(t)^{1-\omega_Z} A_Z(t)^{\beta_Z-1}. \tag{92}$$

Taking the derivative with respect to time one receives

$$\frac{\dot{\mu}_{A_Z}(t)}{\mu_{A_Z}(t)} = \frac{\dot{U}_l(t)}{U_l(t)} + (\theta-\omega_Z)\frac{\dot{P}(t)}{P(t)} + (1-\omega_Z)\frac{\dot{L}_{R,Z}(t)}{L_{R,Z}(t)} + (\beta_Z-1)\frac{\dot{A}_Z(t)}{A_Z(t)}. \tag{93}$$

Research labour in the energy sector. Taking the derivative with respect to $L_{R,E}(t)$ yields

$$\begin{aligned}\frac{\partial \mathcal{H}}{\partial L_{R,E}(t)} &= P(t)^{\theta} U_{L_{R,E}}(t) \\ &\quad + \mu_{A_E}(t)\zeta_E \omega_E \big(L_{R,E}(t)P(t)\big)^{\omega_E-1} P(t) A_E(t)^{1-\beta_E} = 0.\end{aligned}$$

Using $U_{L_{R,E}}(t) = -U_l(t)$ gives

$$P(t)^{\theta} U_l(t) = \mu_{A_E}(t)\zeta_E \omega_E P(t)^{\omega_E} L_{R,E}(t)^{\omega_E-1} A_E(t)^{1-\beta_E}. \tag{94}$$

$$\mu_{A_E}(t) = \frac{U_l(t)}{\zeta_E \omega_E} P(t)^{\theta-\omega_E} L_{R,E}(t)^{1-\omega_E} A_E(t)^{\beta_E-1}. \tag{95}$$

Taking the derivative with respect to time one receives

$$\dot{\mu}_{A_E}(t) = \mu_{A_E}(t)\left[\frac{\dot{U}_l(t)}{U_l(t)} + (\theta-\omega_E)\frac{\dot{P}(t)}{P(t)} + (1-\omega_E)\frac{\dot{L}_{R,E}(t)}{L_{R,E}(t)} + (\beta_E-1)\frac{\dot{A}_E(t)}{A_E(t)}\right]. \tag{96}$$

Productivity in the intermediate sector. Taking the derivative with respect to $A_Z(t)$ yields

$$\begin{aligned}\frac{\partial \mathcal{H}}{\partial A_Z(t)} &= \mu_Y(t) F_{A_Z}(t) \\ &\quad + \mu_{A_Z}(t)\zeta_Z \big(L_{R,Z}(t)P(t)\big)^{\omega_Z}(1-\beta_Z) A_Z(t)^{-\beta_Z} \stackrel{!}{=} \rho \mu_{A_Z}(t) - \dot{\mu}_{A_Z}(t).\end{aligned}$$

Dividing by $\mu_{A_Z}(t)$ gives

$$\rho - \frac{\dot{\mu}_{A_Z}(t)}{\mu_{A_Z}(t)} = \frac{\mu_Y(t)}{\mu_{A_Z}(t)} F_{A_Z}(t) + \zeta_Z \big(L_{R,Z}(t)P(t)\big)^{\omega_Z} (1-\beta_Z) A_Z(t)^{-\beta_Z}. \tag{97}$$

Substituting

$$\frac{\dot{\mu}_{A_Z}(t)}{\mu_{A_Z}(t)} = \frac{\dot{U}_l(t)}{U_l(t)} + (\theta - \omega_Z)\frac{\dot{P}(t)}{P(t)} + (1-\omega_Z)\frac{\dot{L}_{R,Z}(t)}{L_{R,Z}(t)} + (\beta_Z - 1)\frac{\dot{A}_Z(t)}{A_Z(t)}, \tag{98}$$

$$\mu_Y(t) = P(t)^{\theta-1} U_c(t), \tag{99}$$

$$\mu_{A_Z}(t) = \frac{U_l(t)}{\zeta_Z \omega_Z} P(t)^{\theta-\omega_Z} L_{R,Z}(t)^{1-\omega_Z} A_Z(t)^{\beta_Z - 1}, \tag{100}$$

yields

$$\rho - \frac{\dot{U}_l(t)}{U_l(t)} - (\theta - \omega_Z)\frac{\dot{P}(t)}{P(t)} - (1-\omega_Z)\frac{\dot{L}_{R,Z}(t)}{L_{R,Z}(t)} = \omega_Z \zeta_Z \frac{A_Z(t)^{1-\beta_Z}}{\big(P(t)L_{R,Z}(t)\big)^{1-\omega_Z}} \frac{U_c(t)}{U_l(t)} F_{A_Z}(t). \tag{101}$$

Productivity in the energy sector. Taking the derivative with respect to $A_E(t)$ yields

$$\begin{aligned}\frac{\partial \mathcal{H}}{\partial A_E(t)} &= \mu_Y(t) F_{A_E}(t) - \lambda(t) E_{A_E}(t) \\ &\quad + \mu_{A_E}(t) \zeta_E \big(L_{R,E}(t)P(t)\big)^{\omega_E} (1-\beta_E) A_E(t)^{-\beta_E} \stackrel{!}{=} \rho \mu_{A_E}(t) - \dot{\mu}_{A_E}(t).\end{aligned}$$

Dividing by $\mu_{A_E}(t)$ gives

$$\rho - \frac{\dot{\mu}_{A_E}(t)}{\mu_{A_E}(t)} = \frac{\mu_Y(t)}{\mu_{A_E}(t)} F_{A_E}(t) - \frac{\lambda(t)}{\mu_{A_E}(t)} E_{A_E}(t) + \zeta_E \big(L_{R,E}(t)P(t)\big)^{\omega_E} (1-\beta_E) A_E(t)^{-\beta_E}. \tag{102}$$

Substituting eqs. (95) and (96) yields

$$\rho - \frac{\dot{U}_l(t)}{U_l(t)} - (\theta - \omega_E)\frac{\dot{P}(t)}{P(t)} - (1-\omega_E)\frac{\dot{L}_{R,E}(t)}{L_{R,E}(t)} - (\beta_E - 1)\frac{\dot{A}_E(t)}{A_E(t)} = \tag{103}$$
$$\zeta_E P(t)^{\omega_E - 1} L_{R,E}(t)^{\omega_E - 1} A_E(t)^{-\beta_E}$$
$$\left[\omega_E \frac{U_c(t)}{U_l(t)} A_E(t) F_{A_E}(t) - \omega_E \frac{\lambda(t)}{U_l(t)} P(t)^{1-\theta} A_E(t) E_{A_E}(t) + P(t) L_{R,E}(t)(1-\beta_E)\right].$$

and finally

$$\rho - \frac{\dot{U}_l(t)}{U_l(t)} - (\theta - \omega_E)\frac{\dot{P}(t)}{P(t)} - (1-\omega_E)\frac{\dot{L}_{R,E}(t)}{L_{R,E}(t)} = \frac{\omega_E \zeta_E A_E(t)^{1-\beta_E}}{\big(P(t)L_{R,E}(t)\big)^{1-\omega_E}} \frac{U_c(t)}{U_l(t)} \left(F_{A_E}(t) - \frac{\lambda(t) E_{A_E}(t)}{P(t)^{\theta-1} U_c(t)}\right). \tag{104}$$

Population. Taking the derivative with respect to $P(t)$ yields

$$\frac{\partial \mathcal{H}}{\partial P(t)} = \theta P(t)^{\theta-1} U(\cdot) + \mu_Y(t)\big(F_P(t) - c(t)\big) - \lambda(t) E_P(t) + \mu_P(t)\big(n(t) - d\big)$$
$$+ \mu_{A_Z}(t)\frac{\partial \dot{A}_Z(t)}{\partial P(t)} + \mu_{A_E}(t)\frac{\partial \dot{A}_E(t)}{\partial P(t)} \stackrel{!}{=} \rho \mu_P(t) - \dot{\mu}_P(t).$$

Using

$$\frac{\partial \dot{A}_Z(t)}{\partial P(t)} = \zeta_Z \omega_Z L_{R,Z}(t)^{\omega_Z} P(t)^{\omega_Z - 1} A_Z(t)^{1-\beta_Z}, \tag{105}$$
$$\frac{\partial \dot{A}_E(t)}{\partial P(t)} = \zeta_E \omega_E L_{R,E}(t)^{\omega_E} P(t)^{\omega_E - 1} A_E(t)^{1-\beta_E}, \tag{106}$$

together with

$$\mu_Y(t) = P(t)^{\theta-1} U_c(t), \tag{107}$$
$$\mu_P(t) = -P(t)^{\theta-1} \frac{U_{L_n}(t)}{\kappa \psi L_n(t)^{\psi-1}}, \tag{108}$$
$$\frac{\dot{\mu}_P(t)}{\mu_P(t)} = (\theta - 1)\frac{\dot{P}(t)}{P(t)} + \frac{\dot{U}_{L_n}(t)}{U_{L_n}(t)} - (\psi - 1)\frac{\dot{L}_n(t)}{L_n(t)} - \frac{\dot{\kappa}(t)}{\kappa(t)}. \tag{109}$$
$$\mu_{A_Z}(t) = \frac{U_l(t)}{\zeta_Z \omega_Z} P(t)^{\theta - \omega_Z} L_{R,Z}(t)^{1-\omega_Z} A_Z(t)^{\beta_Z - 1}, \tag{110}$$
$$\mu_{A_E}(t) = \frac{U_l(t)}{\zeta_E \omega_E} P(t)^{\theta - \omega_E} L_{R,E}(t)^{1-\omega_E} A_E(t)^{\beta_E - 1}, \tag{111}$$

and noting that

$$\mu_{A_Z}(t)\frac{\partial \dot{A}_Z(t)}{\partial P(t)} = U_l(t)P(t)^{\theta-1}L_{R,Z}(t), \tag{112}$$

$$\mu_{A_E}(t)\frac{\partial \dot{A}_E(t)}{\partial P(t)} = U_l(t)P(t)^{\theta-1}L_{R,E}(t), \tag{113}$$

rearranging yields

$$\begin{aligned}&\theta\frac{\dot{P}(t)}{P(t)} + \frac{\dot{U}_{L_n}(t)}{U_{L_n}(t)} - (\psi-1)\frac{\dot{L}_n(t)}{L_n(t)} - \frac{\dot{\kappa}(t)}{\kappa(t)} \\ &= \rho + \kappa\psi L_n(t)^{\psi-1}\frac{U_c(t)}{U_{L_n}(t)}\left(\theta\frac{U(\cdot)}{U_c(t)} + F_P(t) - c(t) - \frac{\lambda(t)E_P(t)}{P(t)^{\theta-1}U_c(t)} + \frac{U_l(t)}{U_c(t)}\big(L_{R,Z}(t) + L_{R,E}(t)\big)\right).\end{aligned} \tag{114}$$

E.1.3 Optimality Conditions

The optimum with endogenous growth is described by the following seven optimality conditions. The first four are identical to the model with exogenous growth and given by

$$F_{K_Z}(t) - \delta - \rho = -\frac{\dot{U}_c(t)}{U_c(t)} - (\theta-1)\frac{\dot{P}(t)}{P(t)}, \tag{115}$$

$$F_{K_E}(t) - \delta - \rho = -\frac{\dot{U}_c(t)}{U_c(t)} - (\theta-1)\frac{\dot{P}(t)}{P(t)} + \frac{\lambda(t)E_{K_E}(t)}{P(t)^{\theta-1}U_c(t)}, \tag{116}$$

$$F_{L_Z}(t) = -\frac{U_{L_Z}(t)}{U_c(t)}P(t), \tag{117}$$

$$F_{L_E}(t) = -\frac{U_{L_E}(t)}{U_c(t)}P(t) + \frac{\lambda(t)E_{L_E}(t)}{P(t)^{\theta-1}U_c(t)}. \tag{118}$$

The optimality condition for population now has an additional term, taking into account the extra effect on research labor

$$\begin{aligned}&\theta\frac{\dot{P}(t)}{P(t)} + \frac{\dot{U}_{L_n}(t)}{U_{L_n}(t)} - (\psi-1)\frac{\dot{L}_n(t)}{L_n(t)} - \frac{\dot{\kappa}(t)}{\kappa(t)} = \rho + \kappa\psi L_n(t)^{\psi-1}\frac{U_c(t)}{U_{L_n}(t)}\times \\ &\left(\theta\frac{U(\cdot)}{U_c(t)} + F_P(t) - c(t) - \frac{\lambda(t)E_P(t)}{P(t)^{\theta-1}U_c(t)} + \frac{U_l(t)}{U_c(t)}\big(L_{R,Z}(t) + L_{R,E}(t)\big)\right).\end{aligned} \tag{119}$$

Finally, there are two new optimality conditions governing the optimal allocation of research time over time in the two sectors. Research in energy is affected by the energy limit.

$$\rho - \frac{\dot{U}_l(t)}{U_l(t)} - (\theta - \omega_Z)\frac{\dot{P}(t)}{P(t)} - (1-\omega_Z)\frac{\dot{L}_{R,Z}(t)}{L_{R,Z}(t)} = \frac{\omega_Z \zeta_Z A_Z(t)^{1-\beta_Z}}{\big(P(t)L_{R,Z}(t)\big)^{1-\omega_Z}}\frac{U_c}{U_l}F_{A_Z}(t), \quad (120)$$

$$\rho - \frac{\dot{U}_l(t)}{U_l(t)} - (\theta - \omega_E)\frac{\dot{P}(t)}{P(t)} - (1-\omega_E)\frac{\dot{L}_{R,E}(t)}{L_{R,E}(t)} = \frac{\omega_E \zeta_E A_E(t)^{1-\beta_E}}{\big(P(t)L_{R,E}(t)\big)^{1-\omega_E}}\frac{U_c}{U_l}\times \quad (121)$$

$$\left(F_{A_E}(t) - \frac{\lambda(t)E_{A_E}(t)}{P(t)^{\theta-1}U_c(t)}\right).$$

The equations of motion are given by

$$\dot{P}(t) = \big(n(t) - d\big)P(t), \quad (122)$$

$$\dot{K}_Z(t) = I_Z(t) - \delta K_Z(t), \quad (123)$$

$$\dot{K}_E(t) = I_E(t) - \delta K_E(t), \quad (124)$$

$$\dot{A}_Z(t) = \zeta_Z\big(L_{R,Z}(t)P(t)\big)^{\omega_Z}A_Z(t)^{1-\beta_Z}, \quad (125)$$

$$\dot{A}_E(t) = \zeta_E\big(L_{R,E}(t)P(t)\big)^{\omega_E}A_E(t)^{1-\beta_E}. \quad (126)$$

Resource constraint and Kuhn-Tucker Conditions are

$$Y(t) = c(t)P(t) + I_Z(t) + I_E(t), \quad (127)$$

$$\lambda(t) \geq 0, \qquad E(t) \leq \bar{E}, \qquad \lambda(t)\big(E(t) - \bar{E}\big) = 0. \quad (128)$$

The transversality conditions are

$$\lim_{t\to\infty} e^{-\rho t}\mu_Y(t)K_Z(t) = 0, \quad (129)$$

$$\lim_{t\to\infty} e^{-\rho t}\mu_Y(t)K_E(t) = 0, \quad (130)$$

$$\lim_{t\to\infty} e^{-\rho t}\mu_P(t)P(t) = 0, \quad (131)$$

$$\lim_{t\to\infty} e^{-\rho t}\mu_{A_Z}(t)A_Z(t) = 0, \quad (132)$$

$$\lim_{t\to\infty} e^{-\rho t}\mu_{A_E}(t)A_E(t) = 0. \quad (133)$$